Geoscience Frontiers 4 (2013) 583–596

Contents lists available at SciVerse ScienceDirect

China University of Geosciences (Beijing)

Geoscience Frontiers

journal homepage: www.elsevier.com/locate/gsf

Focus paper

Global glaciations and atmospheric change at ca. 2.3 Ga

Haoshu Tang [a,b], Yanjing Chen [b,c,*]

[a] State Key Laboratory of Ore Deposit Geochemistry, Institute of Geochemistry, Chinese Academy of Sciences, 46 Guanshui Road, Guiyang 550002, China
[b] Key Laboratory of Orogen and Crust Evolution, Peking University, Beijing 100871, China
[c] Key Laboratory of Mineralogy and Metallogeny, Guangzhou Institute of Geochemistry, Chinese Academy of Sciences, Guangzhou 510640, China

ARTICLE INFO

Article history:
Received 1 May 2012
Received in revised form
4 February 2013
Accepted 7 February 2013
Available online 26 February 2013

Keywords:
Global glaciation
Earth's environmental change
Great Oxidation Event
Lithostratigraphy
Geochronology

ABSTRACT

This paper compiles lithostratigraphic and geochronological data obtained for the Palaeoproterozoic glacial diamictite-bearing successions, and thereby provides insights into understanding the geological processes causing the Huronian Glaciation Event. The majority of evidence for appearances of this glaciation event can be related to the Kenorland supercontinent breakup, allied to significant atmospheric change, as well as blooms of biogeochemical oxygenic photosynthesis. In this paper, the Huronian Glaciation Event is constrained to have occurred synchronously during 2.29–2.25 Ga, accompanied by dramatic environmental changes characteristic of the Great Oxidation Event which includes the pre-2.3 Ga hydrosphere oxidation and the post-2.3 Ga atmosphere oxygenation.

1. Introduction

The Archaean/Palaeoproterozoic transition witnessed dramatic changes in Earth's history which include several environmental oscillations and the emergence of an aerobic Earth System (e.g., Chen, 1990; Chen and Su, 1998; Bekker et al., 2004, 2010; Bekker and Kaufman, 2007; Frei et al., 2009; Holland, 2009; Konhauser et al., 2009, 2011; Lyons and Reinhard, 2009; Tang et al., 2011, 2012; Young, 2012, 2013; Zhai and Santosh, 2013). One of the earliest significant events known from this transition is the sharp drop of volcanism (Holland, 2002) and temperature resulting in the formation of stably normal sedimentary basins over the world and the rapid onset of global glacial event. Palaeoproterozoic glaciogenic rocks have been known since the beginning of the last century in almost every continent, including North America, Fennoscandia, South Africa, Western Australia, South America, and India (Table 1; Young, 1970, 2002; Hambrey and Harland, 1981; Bekker et al., 2001, 2005, 2006; Ojakangas et al., 2001; Melezhik, 2006; Eriksson et al., 2011; Strand, 2012; and references therein). This is the oldest glaciation known of global significance and has been termed as the "Huronian Glaciation" after the best-studied example from the Huronian Supergroup in Canada (Young, 1970; Miall, 1983; Young et al., 2001). It was followed shortly after the 2450 Ma breakup of the Kenorland/Superia supercontinent (Aspler and Chiarenzelli, 1998; Bekker and Eriksson, 2003; Eyles, 2008) and prevailed at some time between ca. 2.4 (possibly 2.45 Ga) and 2.2 Ga, with up to three possible glacial horizons, couched within a "Snowball Earth model" (Hoffman et al., 1998; Kirschvink et al., 2000) and the "Great Oxidation Event" (GOE). The GOE is widely accepted to have occurred during 2.3–1.8 Ga (Holland, 1994, 2002; Rye and Holland, 1998; Kasting and Siefert, 2002; Farquhar et al., 2010; Tang et al., 2011, 2013; Lai et al., 2012) and recently traced to have begun at some time between 2.4 and 2.3 Ga (e.g., Karhu and Holland, 1996; Bekker et al., 2004; Canfield, 2005; Anbar et al., 2007; Holland, 2009).

The causes and timing of the Huronian Glaciation Event (abbreviated to HGE hereafter), as well as the global extent of ice cover are still controversial (Young, 1991; Evans et al., 1997; Evans, 2003; Kopp et al., 2005). It remains possible that the glaciation was diachronous in different areas, rather than a simultaneous and catastrophic event as implicit within the Snowball Earth model (Eriksson et al., 2011). Thus, this paper compiles and reviews the Palaeoproterozoic glacial records in different cratons, further

* Corresponding author. Key Laboratory of Orogen and Crust Evolution, School of Earth and Space Sciences, Geology Department, Peking University, Room 3511, Building 2 of Yifu, Beijing 100871, China. Tel.: +86 1370 121 0355.

Peer-review under responsibility of China University of Geosciences (Beijing)

Production and hosting by Elsevier

1674-9871/$ – see front matter © 2013, China University of Geosciences (Beijing) and Peking University. Production and hosting by Elsevier B.V. All rights reserved.
http://dx.doi.org/10.1016/j.gsf.2013.02.003

Table 1
Compilation of the reported Palaeoproterozoic diamictite units in the world.

Continent	Name or strata	Geography or locality	Age (Ma)	References
N. America	Gowganda Fm., Cobalt Gp., Huronian SGp.	45°40′–48°40′ N, 79°–85° W; Ontario, Canada	2450 –2217.5	Krogh et al. (1984), Andrews et al. (1986)
N. America	Bruce Fm., Quirke Lake Gp., Huronian SGp.	45°40′–48°40′ N, 79°–85° W; Ontario, Canada	2450 –2217.5	Krogh et al. (1984), Andrews et al. (1986)
N. America	Ramsay Lake Fm., Hough Lake Gp., Huronian SGp.	45°40′–48°40′ N, 79°–85° W; Ontario, Canada	2450 –2217.5	Krogh et al. (1984); Andrews et al. (1986)
N. America	Chibougamau Fm.	49°40′–50°15′ N, 74°40′–73°50′ W; Quebec, Canada	2500–1800	Frakes (1979), Hambrey and Harland (1981)
N. America	Padlei Fm., Hurwitz Gp.	61°–62°30′ N, 95°–99° W; Northwest Territories, Canada	2300–2100	Frakes (1979), Hambrey and Harland (1981)
N. America a	Northern Black Hills	43°50′–44°07′ N, 103°20′–103°45′ W; South Dakota, USA	2559–1870	Dahl et al. (1999)
N. America	Bottle Creek, Singer Peak Fm., Snowy Pass Gp.	Snowy Pass Group, Sierra Madre Mountains, Wyoming, USA	<2450	Frakes (1979), Hambrey and Harland (1981)
N. America	Headquarters Fm., Lower Libby Creek Gr., Snowy Pass SGp.	41°–41°30′ N, 107°15′–106°15′ W, Medicine Bow Mountains, Wyoming, USA	2451–2000	Premo and Van Schmus (1989), Cox et al. (2000)
N. America	Vagner Fm., Deep Lake Gp., Snowy Pass SGp.	41°–41°30′ N, 107°15′–106°15′ W, Medicine Bow Mountains, Wyoming, USA	2451–2000	Premo and Van Schmus (1989), Cox et al. (2000)
N. America	Campbell Lake Fm, Deep Lake Gr., Snowy Pass SGp.	41°–41°30′ N, 107°15′–106°15′ W, Medicine Bow Mountains, Wyoming, USA	<2451 ± 9	Premo and Van Schmus (1989)
N. America	Fem Creek Fm., Chocolay Gp., Marquette Range SGp.	Menominee and Iron River–Crystal Falls Ranges, Amasa Uplift, WI and MI, USA	2302–2115	Bekker et al. (2006), Vallini et al. (2006)
N. America	Enchantment Lake Fm., Chocolay Gp., Marquette Range SGp.	45°49′–46°30′ N, 87°30′–88°05′ W; Marquette Trough, Upper Peninsula Michigan, USA	2288–2131	Bekker et al. (2006), Vallini et al. (2006)
Africa	Witwatersrand SGp.	South Africa	2600–2300	Frakes, 1979; Hambrey and Harland, 1981
Africa	Makganyene Diamictite, Postmasburg Group	28°47′ S, 23°15′ E; Griqualand West Basin, South Africa	2415–2222	Cornell et al. (1996), Gutzmer and Beukes (1998), Bau et al. (1999)
Africa	Boshoek Fm, Lower Pretoria Group, Transvaal SGp.	25°50′ S, 28°25′ E; Transvaal Basin, South Africa	2316–2249	Dorland (2004), Hannah et al. (2004)
Africa	Duitschland Fm, Lower Pretoria Group, Transvaal SGp.	25°50′ S, 28°25′ E; Transvaal Basin, South Africa	2480–2316	Pickard (2003), Hannah et al. (2004)
Australia	Meteorite Bore Mb., Turee Creek Group	22°55′ S, 117° E; Hamersley basin, Western Australia	2209–2449	Barley et al. (1997), Trendall et al. (1998), Pickard (2002)
Antarctica	Widdalen Fm.	71°51′ S, 2°43′ W or 71°05′ S, 2°21′ W	>1700	Frakes (1979), Hambrey and Harland (1981)
Asia	Gangau tillites	79°07′–79°55′ E, 24°20′–24°40′ N; Central India	2600–1850	Frakes (1979), Hambrey and Harland (1981)
Asia	Sanverdam tillites	74°50′–73°10′ E, 15°30′–15°05′ N; South India	2600–2200	Frakes (1979), Hambrey and Harland (1981)
Europe	Sakukan tillites	Baikal, Russia	2640–1950	Melezhik and Fallick (1996), Melezhik et al. (1997b)
Europe	Lammos tillites	68° N, 30° E; Kola Peninsula, Russia	>1900	Melezhik and Fallick (1996), Melezhik et al. (1997b)
Europe	Partanen tillites	Southern Karelia, Russia	2150–1900	Melezhik and Fallick (1996), Melezhik et al. (1997b)
Europe	Sarioli tillites, Karelian Sgp.	Eastern Baltic Shield, Russia	2455–2180	Melezhik and Fallick (1996), Melezhik et al. (1997b)

constrains the time of glaciation and attempts to relate to other secular changes including positive $\delta^{13}C_{carb}$.

2. Geology and timing of typical Palaeoproterozoic glacial records

Archaean plate reconstructions show the assembly of two supercontinents (Aspler and Chiarenzelli, 1998), the Northern Supercontinent (Kenorland/Superia) and the Southern Supercontinent. The former is composed of the North American, Fennoscandian and possibly Siberian shields (Williams et al., 1991). The latter is poorly constrained and likely includes the Kaapvaal, Pilbara, Zimbabwe, São Francisco and Indian cratons (Cheney, 1996; Bleeker, 2003; De Kock et al., 2009a). Both supercontinents experienced protracted breakup driven by inferred mantle plumes and associated intraplate rifting (Aspler and Chiarenzelli, 1998; Bekker and Eriksson, 2003; Zhong et al., 2007; Eyles, 2008). Breakup was shortly followed by the onset of "icehouse" conditions in the Palaeoproterozoic. Hambrey and Harland (1981) documented at least three discrete glacial successions within the Palaeoproterozoic sedimentary record of ~2.45–2.22 Ga (Table 1; Fig. 1A–G). The lowermost glacial record is separated from the continental flood-basalts by a ~2000 m thick, rift-related, siliciclastic succession, and the youngest glaciogenic association is older than 2.22 Ga (Young et al., 2001; Long, 2004).

2.1. North America

In North America, Palaeoproterozoic glaciogenic deposits are present in the Marquette Range Supergroup in Michigan (Fig. 1A), the Huronian Supergroup in Ontario (Fig. 1B), and the Snowy Pass Supergroup in Wyoming (Fig. 1C), as well as in their equivalent successions in northern Quebec and Northwest Territories (Ojakangas, 1988). The best preserved example is from the Huronian Supergroup of Canada (Fig. 1B), which contains three glaciogenic units from the lowermost Ramsey Lake Formation, through Bruce Formation in the middle, and to the uppermost Gowganda Formation, inter-bedded with the shales, carbonate rocks and non-glacial fluvial-deltaic clastic sediments (Fralick and Miall, 1989; Young, 1991; Sekine et al., 2011). The Espanola Formation (Fig. 1B) was ever suggested to be cap carbonates with $\delta^{13}C_{carb}$ values ranging from −4.0‰ to 0.8‰ (Bekker et al., 2005).

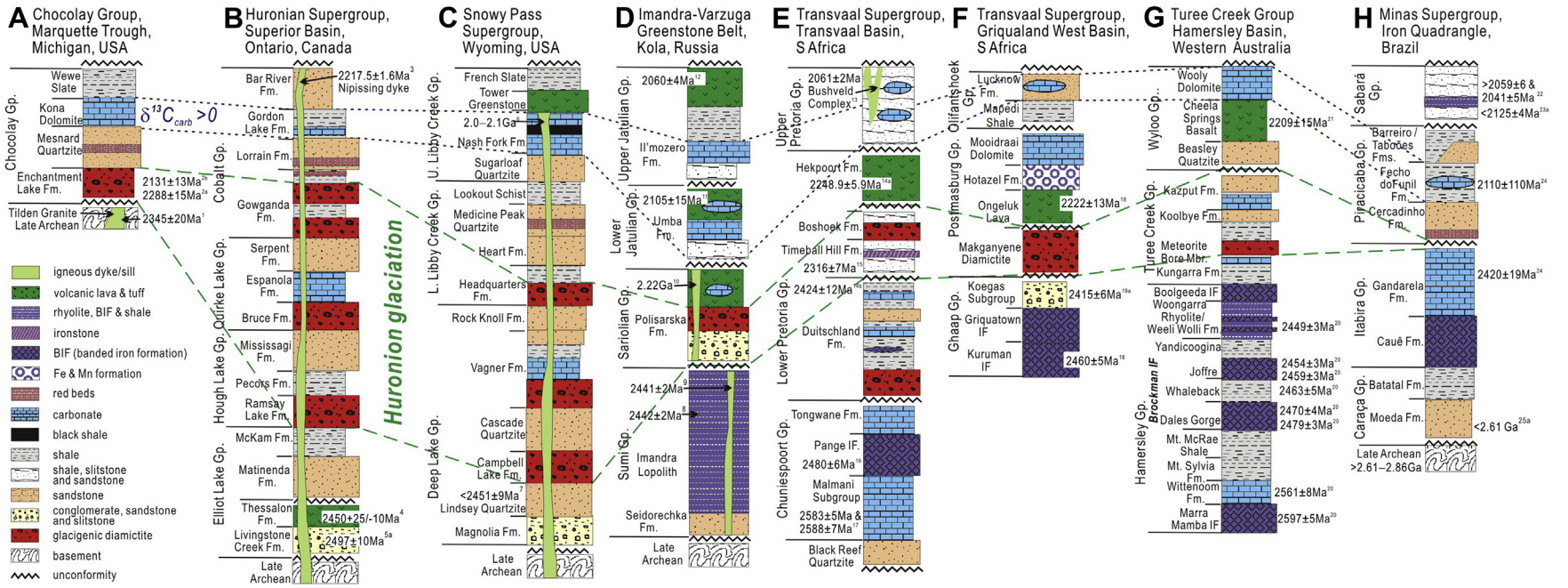

Figure 1. Stratigraphic correlation of the Huronian glaciations in the world (compiled from: Young, 1970, 2002; Miall, 1983; Halls and Bates, 1990; Melezhik and Sturt, 1994; Barley et al., 1997; Heaman, 1997; Vogel et al., 1998; Martin, 1999; Bekker et al., 2001, 2005, 2006; Ojakangas et al., 2001; Young et al., 2001; Lindsay and Brasier, 2002; Pickard, 2003; Hannah et al., 2004; Long, 2004; Melezhik, 2006; Bekker and Kaufman, 2007; Eriksson et al., 2011; and references therein). Notations to ages: 1. zircon TIMS U-Pb age (Hammond, 1976); 2a. detrital zircon U-Pb age, suggesting maximum age of deposition (Vallini et al., 2006); 2b. hydrothermal xenotime age, suggesting minimum age of deposition (Vallini et al., 2006); 3. baddeleyite TIMS U-Pb age (Andrews et al., 1986); 4. zircon TIMS U-Pb age for volcanic rocks (Krogh et al., 1984); 5. detrital zircon U-Pb age (Rainbird and Davis, 2006); 6. zircon and baddeleyite TIMS U-Pb ages (Premo and Van Schmus, 1989; Cox et al., 2000); 7. detrital zircon TIMS U-Pb age (Premo and Van Schmus, 1989); 8. zircon TIMS U-Pb age for volcanic rocks (Amelin et al., 1995); 9. zircon SHRIMP U-Pb age for basalt lava (Puchtel et al., 1996); 10. cited from Hanski et al. (2001); 11. zircon U-Pb age (Huhma, 1986); 12. zircon U-Pb age (Melezhik et al., 1997a); 13. zircon U-Pb age (Walraven, 1997); 14a. zircon U-Pb age (Dorland, 2004); 14b. detrital zircon U-Pb age (Dorland, 2004); 15. diagenetic pyrite Re-Os isochron age (Hannah et al., 2004); 16. zircon SHRIMP U-Pb age for volcanic ash beds (Pickard, 2003); 17. zircon SHRIMP U-Pb age for ash beds (Martin et al., 1998); 18. whole rock Pb-Pb isochron age (Cornell et al., 1996); 19. detrital zircon U-Pb age (Gutzmer and Beukes, 1998); 20. zircon SHRIMP U-Pb age (Trendall et al., 1998); 21. zircon SHRIMP U-Pb age (Barley et al., 1997); 22. titanite U-Pb age (Noce et al., 1998); 23. detrital zircon U-Pb age (Machado et al., 1992); 24. carbonate Pb-Pb isochron age (Babinski et al., 1995); 25. zircon SHRIMP U-Pb age (Endo et al., 2002); 26. compiled from Machado et al. (1992, 1996), Machado and Carneiro (1992), Chemale et al. (1994), Noce et al. (1998), and Endo et al. (2002).

The Huronian Supergroup is subdivided by unconformities into the Elliot Lake, Hough Lake, Quirke Lake and Cobalt groups in ascending sequence (Fig. 1B). The Elliot Group is the only one stratigraphic unit without diamictite. It rests unconformably on the Archaean basement and has been deposited in a rift setting possibly connected with an ocean to the east (Young et al., 2001). Locally preserved palaeosols at the base of the Elliot Group are reduced (Prasad and Roscoe, 1996), and the Livingstone Creek and Matinenda formations contain uraniferous and pyriferous conglomerates, which indicate that the atmospheric $p(O_2)$ is extremely low (Mossman and Harron, 1983; Chen, 1990, 1996). The shale samples from the McKam Formation (Fig. 1B) do not show any Eu-depletion (Taylor and McLennan, 1985), suggesting an anoxic sedimentary environment (Chen, 1996 and references therein). Moreover, both the Matinenda and McKam formations have high CIA (chemical index of alteration) values which suggest a warm and humid climate (Nesbitt and Young, 1982). Therefore, the environment before the Huronian glaciation was anoxic. The Cobalt Group, starting with the Gowganda Formation (Fig. 1B), comprising the uppermost unit of the Huronian Supergroup, was deposited on a passive margin (Young et al., 2001). The upper Gowganda Formation of the Cobalt Group contains deltaic mudstones and sandstones, and is overlain by mature quartzites of the fluvial Lorrain and tidally-influenced Bar River formations. Unaltered feldspar grains are present in the lower part of the Lorrain Formation, while Al-rich quartzites (containing pyrophyllite, sericite, kaolinite and diaspore) in the middle and upper parts of the Lorrain Formation imply deep weathering in a warm and humid climate (Chandler, 1984). The Lorrain Formation and the Bar River Formation are separated by a thinly inter-bedded succession of varicoloured and silicified mudstone, siltstone, sandstone, and rare carbonate of the Gordon Lake Formation. The Cobalt Group provides evidence for an oxygenated atmosphere, including red beds of the Lorrain Formation and the upper Gowganda Formation (Young et al., 2001), an oxidized Ville Marie palaeosol below the Lorrain Formation (Rainbird et al., 1990; Panahi et al., 2000), pseudomorphs of anhydrite (oxidative sulphur) in the Gordon Lake Formation (Chandler, 1988), and remarkably negative sedimentary Eu anomalies (Taylor and McLennan, 1985; Chen, 1996).

A divergent continental margin, which developed on the south-facing edge of the Superior Craton and was later subjected to a collisional orogeny, has been suggested as the tectonic setting for the Huronian sediments (Young and Nesbitt, 1985; Fralick and Miall, 1989). The basal conglomerate of the Livingstone Creek Formation gives a detrital zircon U-Pb age of 2497 ± 10 Ma (Rainbird and Davis, 2006), and the volcanic rocks of the Thessalon Formation yield a zircon TIMS U-Pb age of 2450 + 25/−10 Ma (Krogh et al., 1984), indicating that the lower portion of the Elliot Lake Group was deposited between 2.5 and 2.45 Ga. A Rb-Sr isochron age of 2330 Ma for the volcanic tuffs from the McKam Formation of the topmost Elliot Lake Group is widely accepted (Taylor and McLennan, 1985), suggesting that the HGE was not earlier than 2.33 Ga. The whole Huronian Supergroup is cut by the Nipissing dykes that yield baddeleyite TIMS U-Pb age of 2217.5 ± 1.6 Ma (Andrews et al., 1986), indicating that the HGE occurred before 2.22 Ga.

In USA, the Chocolay Group of the Marquette Range Supergroup (Fig. 1A) along the southern shore of the Lake Superior in Michigan and Wisconsin is lithostratigraphically correlated with three upper groups of the Huronian Supergroup (Bekker et al., 2006). The Enchantment Lake Formation is lowest unit of the Chocolay Group, unconformably overlying the Archaean basement in the Upper Peninsula of Michigan. It comprises of glacial diamictites and is overlain by the Mesnard quartzites, Kona dolomites and Wewe slates in ascending sequence. The Tilden granite cutting the Archaean Compeau Gneiss in Marquette area (Fig. 1A) yielded zircon U-Pb age of 2345 ± 20 Ma, which was taken as the maximum age of the Chocolay Group (Hammond, 1976). Detrital zircon grains and hydrothermal xenotime crystals from the diamictites yield SHRIMP U-Pb ages of 2288 ± 15 Ma and 2131 ± 13 Ma, respectively (Vallini et al., 2006), well bracketing the depositional duration of the glaciation event.

The Snowy Pass Supergroup in Wyoming Craton, USA, can be better correlated with the Huronian Supergroup (Fig. 1B, C; Bekker et al., 2005). It either unconformably overlies or structurally contacts with the late Archaean basement, and includes the Deep Lake Group, the lower Libby Creek Group and the upper Libby Creek Group in ascending sequence. Three glaciogenic units can be observed in two lower groups, which are lithologically sandwiched with quartzites, metapelites and thin-bedded carbonates. Both the Deep Lake Group and the lower Libby Creek Group were deposited in rift and passive margin settings. The Deep Lake Group starts with a fluvial rift deposition, characterized by quartz-pebble conglomerates containing detrital pyrite and uraninite (Magnolia Formation), indicating a low $p(O_2)$ atmosphere. A transition from intracratonic rift to open marine settings coincided with deposition of the Vagner Formation (Karlstrom et al., 1983). The lower Libby Creek Group possibly records a transition from passive margin to foredeep (Karlstrom et al., 1983) or dissection of a mature passive margin (Bekker and Eriksson, 2003). The youngest glacial diamictite unit is overlain by thick, mature, Al-rich and haematite-bearing quartzites (Medicine Peak Quartzite), and carbonate units (Nash Fork Formation) with positive $\delta^{13}C$ anomalies (Bekker et al., 2003a).

The detrital zircon grains from the clastic sediments beneath the lowest diamictite unit at Sierra Madre area yielded TIMS U-Pb age of 2451 ± 9 Ma (Premo and Van Schmus, 1989), constraining the maximum glaciation age to be <2.45 Ga. Zircon and baddeleyite from the tholeiitic gabbros intruding the Deep Lake Group at Sierra Madre and Laramie areas yield TIMS U-Pb ages of 2.09–2.01 Ga (Premo and Van Schmus, 1989; Cox et al., 2000). This shows that the glaciation in Wyoming Craton occurred in the bracket of 2.45–2.1 Ga.

2.2. Fennoscandian

In the Fennoscandian Shield, the Palaeoproterozoic rocks are subdivided into Sumi, Sarioli, lower Jatulian, upper Jatulian, Ludikovi, and Kalevi groups in younging sequence (Melezhik et al., 1997a). The Sumi Group consists of basaltic pyroclastics, tuffs, redeposited coarse volcanic clastics, and basaltic subaerial lavas that can be >3000 m thick in the Imandra–Varzuga Greenstone Belt (Melezhik et al., 1997b). The volcanic rocks in the Sumi Group are considered to be continental flood-basalts (Puchtel et al., 1996, 1997; Heaman, 1997) coeval and comagmatic with the 2505–2432 Ma layered gabbro complexes (Melezhik and Sturt, 1994; Amelin et al., 1995; Vogel et al., 1998). The rift-related Sumi Group volcanic rocks are separated from the overlying Sariolian Group sedimentary successions by a regional unconformity which can be traced throughout Fennoscandia (Sturt et al., 1994). It was estimated that there were at least 2–3 km of erosion occurred prior to deposition of the Sarioli units, because clasts of the layered gabbro intrusions are incorporated in the conglomerates of the Sariolian Group and petrological evidence suggests that the intrusions crystallized at depths of 2–3 km (Latypov et al., 1999).

The glaciogenic units in the Polisarska Formation (Fig. 1D) of the Imandra–Varzuga Greenstone Belt in the Kola Peninsula and the Urkkavaara Formation of the North Karelia Schist Belt in Finland are associated with the Sariolian Group sedimentary successions (Ojakangas et al., 2001) and their equivalents such as the

Neverskrukk Formation in the Pechenga Greenstone Belt and the Sompujärvi Formation in the Perapähja Schist Belt (Melezhik, 2006). These units consist of polymict conglomerates, gritstones, sandstones, diamictites and varve-like sedimentary rocks with dropstones interpreted as glaciomarine (Marmo and Ojakangas, 1984; Strand and Laajoki, 1993; Ojakangas et al., 2001).

The glaciation event can be constrained between 2441 ± 2 Ma (the age of the Sumi volcanic rocks; Amelin et al., 1995; Puchtel et al., 1996) and 2221 Ma (the age of diabase dyke intruding the Sariolian Group; Hanski et al., 2001). In addition, the duration of the unconformity between the Sumi Group and the Sariolian Group (Fig. 1D) was inferred between 2.44 Ga and 2.33 Ga (Melezhik, 2006). The latter limit comes from a whole-rock Rb-Sr isochron age of 2330 ± 38 Ma dated for volcanic rocks in the Pechenga Greenstone Belt (Balashov et al., 1994) that was supposed comparable to the Sariolian Group (Melezhik, 2006).

In the North Karelia Schist Belt, diamictite, varve-like sediment with dropstones and graded sandstone form the ~60 m Urkkavaara Formation (Marmo and Ojakangas, 1984). These rocks were deposited on ~250 m thick conglomerates which mark a regional high-angle unconformity with underlying units. The depositional age of the Urkkavaara Formation remains poorly constrained but was suggested to correlate with a part of the Sariolian succession (Melezhik et al., 1997a; Melezhik, 2006).

The deposition of Sariolian sediments was followed by an intensive weathering period that resulted in the development of palaeosols throughout the Fennoscandian Shield (Melezhik et al., 1997a). These palaeosols, separating the Sariolian and lower Jatulian successions, can be observed at the areas developed with the Jatulian Group (Marmo, 1992). The internal boundary between the lower Jatulian and upper Jatulian groups can be estimated between 2115 ± 6 Ma (zircon U-Pb age of the Koljola diabase dike; Pekkarinen and Lukkarinen, 1991) and 2105 ± 15 Ma (zircon U-Pb age of the Oravaara basalts; Huhma, 1986) at Kiihtelysvaara. The 2.22–2.06 Ga Jatulian successions in the Fennoscandian Shield distribute in an area of >800,000 km^2 and show remarkably positive $\delta^{13}C_{carb}$ excursion (Schidlowski et al., 1976; Melezhik and Fallick, 1996).

The boundary between the upper Jatulian Group and the overlying Ludikovian Group is widely marked by an abrupt change from 'red beds' to organic carbon-bearing sediments (Melezhik et al., 1997a). The age for the Jatuli–Ludikovi boundary can be obtained from a number of areas; for instance, from the Kittila–Kolari Greenstone Belt is based on the zircon U-Pb age of 2060 ± 4 Ma dated for the Riikonkoski albite gabbro (Melezhik et al., 1997a), which constrains the earliest development of organic carbon-bearing sediments.

2.3. South Africa

Attenuation of the Southern Supercontinent involved crust- and mantle-driven magmatism followed by rifting (Melezhik, 2006). In South Africa, this is manifested by an igneous event forming extensive mafic tuffs aged 2470–2430 Ma (Jones et al., 1975; Hamilton, 1977), almost coeval with the deposition of 2480–2465 Ma banded iron formations (Bekker et al., 2001; and references therein).

The Transvaal Supergroup sedimentary and volcanic rocks were deposited in an epicontinental setting over an area of >500,000 km^2 on the Kaapvaal Craton from ca. 2.6 Ga to 2.0 Ga (Walraven et al., 1990; Bau et al., 1999; Buick et al., 2001). They are mainly preserved in the Transvaal (eastern or northeastern) (Fig. 1E) and Griqualand West (or southwestern) basins (Fig. 1F; Beukes, 1986; Button, 1986; Eriksson et al., 2011). In the Transvaal Basin, the Transvaal Supergroup comprises, in ascending sequence (Fig. 1E), (1) the protobasinal sediments underlying the Chuniespoort Group, (2) the Chuniespoort Group composed of marine-platform jaspilites, banded iron formations, dolostones and quartzites (Bekker et al., 2001), and (3) the uppermost, shallow-marine to fluvial Pretoria Group unconformably overlying the Chuniespoort Group (Tankard et al., 1982; Buick et al., 1998). The Transvaal Supergroup was intruded by mafic rocks of the Bushveld Complex at 2061 ± 2 Ma (Walraven, 1997). The Duitschland Formation, the lowest unit of the Pretoria Group (Fig. 1E), is dominated by marls, mudrocks, dolostones and limestones, with minor thin beds of quartzite and conglomerate, as well as the glaciogenic diamictite bed at the base (Frauenstein et al., 2009; Eriksson et al., 2011). Detrital zircon grains from the uppermost unit of the Duitschland Formation yield U-Pb age of 2424 ± 12 Ma (Dorland, 2004); whilst the unconformably overlying the Timeball Hill (or Rooihoogte) Formation shales yield diagenetic pyrite Re-Os isochron age of 2316 ± 7 Ma (Bekker et al., 2004; Hannah et al., 2004). This shows that the diamictites in the Duitschland Formation must be deposited in the span of 2424–2316 Ma, obviously earlier than those in North America, and unlikely correlated with the HGE.

The Boshoek Formation is dominated by glacial diamictites. It overlies the Timeball Hill Formation shales aged 2316 ± 7 Ma (Hannah et al., 2004), and is covered by the Hekpoort Formations flood basalts aged 2248.9 ± 5.9 Ma (Dorland, 2004). The glaciation time, therefore, is constrained in the period of 2.32–2.25 Ga, well coeval to the HGE in North America.

In the Griqualand West Basin in the Northern Cape Province, the Transvaal Supergroup has been subdivided into the basal Ghaap Group, middle Postmasburg Group, and overlying Olifantshoek Group (Fig. 1F), corresponding to the Chuniespoort, lower Pretoria and upper Pretoria Groups in the Transvaal Basin, respectively. The Postmasburg Group includes four different lithologic units (Fig. 1F), with the lowest Makganyene Formation being composed of diamictites (Polteau et al., 2006). The Makganyene Formation is variable in thickness up to 500 m, but 3–70 m in general. It comprises mostly of massive and coarsely bedded diamictites, with subordinate lenticular conglomerates, sandstones and mudrocks (locally varved) (Polteau et al., 2006). The diamictite formation is unconformably overlain by the Ongeluk flood basalts aged 2222 ± 13 Ma (Cornell et al., 1996), and unconformably overlies the Ghaap Group (Altermann and Nelson, 1998) with detrital zircon U-Pb age of 2415 ± 6 Ma (Gutzmer and Beukes, 1998), suggesting that the glaciation occurred in the time span of 2.41–2.22 Ga.

2.4. Western Australia

In Australia (Fig. 1G), a 2449 Ma large igneous province was developed equatorially (Evans, 2003) and accompanied by the largest Palaeoproterozoic banded iron formation (Barley et al., 1997; Pickard, 2003). The Palaeoproterozoic Hamersley basin lies close to the southern margin of the Pilbara Block (Trendall, 1990; Blake and Barley, 1992) and accommodates the Hamersley, Turee Creek and Wyloo groups (Fig. 1G). The Hamersley Group is well known for the development of banded iron formation (Trendall and Blockley, 1970) and some of the Earth's earliest platform carbonates (2.6–2.5 Ga; Simonson et al., 1993). It developed in a rift setting, and consequently, contains lots of biogeochemical sediments, volcanic rocks fine-grained clastic rocks. The Turee Creek Group records the transition from a passive margin to a foreland basin setting (Tyler and Thorne, 1990) and upwardly includes the Kungarra, Koolbye and Kazput Formations (Fig. 1G). The Meteorite Bore Member of the Kungarra Formation was determined to be glaciogenic diamictites (Lindsay and Brasier, 2002). To date, no isotope age has been reported for the diamictites and the whole Turee Creek Group. However, the Turee Creek Group overlies the

Hamersley Group whose rhyolite yields zircon SHRIMP U-Pb age of 2449 ± 3 Ma (Trendall et al., 1998; Pickard, 2002), suggesting that the glaciation was not earlier than 2.45 Ga. The group is overlain by the Wyloo Group whose Cheela Springs basalt formation yields SHRIMP zircon U-Pb age of 2209 ± 15 Ma (Barley et al., 1997), indicating that the glaciation ended before 2.21 Ga.

2.5. Brazil

In Brazil (Fig. 1H), deposition of the Minas Supergroup was initiated with rifting and breakup of the eastern margin on the Archaean platform and ended with the Transamazonian Orogeny (Marshak and Alkmim, 1989). The late stage of the Transamazonian Orogeny was constrained by titanite ages of 2059 ± 6 Ma and 2041 ± 6 Ma (Machado et al., 1992; Noce et al., 1998) and by 2125 ± 4 Ma U-Pb age of detrital zircon from the overlying orogenic Sabará Group (Machado et al., 1992). The Minas Supergroup includes the Caraças, Itabira, and Piracicaba groups (Bekker et al., 2003b). A minimum age of the Itabira Group is constrained by the carbonate Pb-Pb age of 2420 ± 19 Ma obtained for the Gandarela Formation (Babinski et al., 1995).

There is a wide sedimentary discontinuity between the Itabira and Piracicaba Groups. Evidence for erosional unconformity includes locally angular contact with the Gandarela Formation, Itabira Group, and locally preserved regolith at the top of the Gandarela Formation containing red or variegated fine-grained lenticular rocks (Maxwell, 1972). Phyllites in the basal part of the formation contain large amounts of kyanite which represents a reworked Al-rich regolith above the unconformity (Herz and Dutra, 1964). Herringbone cross bedding, planar bedding, soft-sediment deformation structures, and ripple marks are abundant in quartz arenites of the overlying Cercadinho Formation, indicating a shallow-marine, tidally-influenced sedimentary environment (Romano, 1989). The carbonate Pb-Pb age of 2110 ± 110 Ma for the Fecho do Funil Formation, Piracicaba Group, was related to a metamorphic overprint due to the Transamazonian Orogeny (Babinski et al., 1995). Therefore, during 2.42–2.11 Ga, the São Francisco Craton, southeastern Brazil, was subjected to an erosion, which probably resulted in the absence of glacial diamictites (Bekker et al., 2003b).

3. Timing of the Huronian Glaciation Event

3.1. Discreteness of glacial deposits

The Palaeoproterozoic glaciogenic rocks have been preserved in almost every continent, but the occurrence of glacial diamictites is discrete in different continents and even within a single craton. For example, there are three to four glacial intervals in the North American continent (Fig. 1B, C), but in other continents (e.g., South Africa or Western Australia, Fig. 1F, G) only one diamictite unit can be observed. Moreover, in the Minas Supergroup of São Francisco Craton (Brazil), no glaciogenic diamictite bed has been recognized yet. As shown in Fig. 1B and C, the sedimentation of the Huronian Supergroup in southern Ontario and the Snowy Pass Supergroup in Wyoming are continuous, and consequently, the diamictites are well observed. At least three correlating levels of glacial diamictites are recognized in both areas (Ojakangas, 1988; Young, 1991; Bekker et al., 2005).

The Enchantment Lake diamictite unit and its hosting Chocolay Group in Michigan can be well correlated with the Cobalt Group in Ontario and Libby Creek Group in Wyoming in both lithology and stratigraphy (Fig. 1A, B; Young, 1973; Ojakangas et al., 2001; Argast, 2002; Bekker et al., 2006). However, the glacial diamictites of the Enchantment Lake Formation are confined to the eastern part of the Chocolay Group outcrop area in the Upper Peninsula of Michigan and unconformably overlie the Archaean basement. The other two lower diamictite units developed in Ontario and Wyoming are absent in this area. This may be related to the erosion prior to the deposition of the Enchantment Lake Formation (Morey and Southwick, 1995); and alternately, the other two lower diamictite units are combined into the Enchantment Lake Formation. Similarly, there is an unconformity or sedimentary discontinuity between the Archaean to lowermost Palaeoproterozoic basements (>2.4 Ga) and the overlying glaciogenic diamictite successions or equivalents in the Fennoscandian Shield, Kaapvaal Craton, São Francisco Craton and Pilbara Block (Fig. 1). The ~300 Ma (from 2420 to 2110 Ma) sedimentary discontinuity between the Itabira Group and the Piracicaba Group in the São Francisco Craton entirely span the Huronian glaciation period. Thus, in spite of the incompleteness or absence of the glacial records in some cratons, which could be correlated with unconformities due to glacio-eustatic sea-level fall, it is possible to correlate the Palaeoproterozoic glacial diamictites (Fig. 2 and Table 2). It can also be concluded that the Huronian Glaciation Event was likely synchronous all over the world (Fig. 2 and Table 2).

3.2. Timing of the Huronian Glaciation Event

Bekker et al. (2001, 2005) proposed that the diamictites in Gowganda Formation in Canada were temporally equivalent to the Boshoek Formation (or included in the Timeball Hill Formation) and Makganyene Formation in South Africa. In contrast, Kopp et al. (2005) suggested that the Boshoek–Makganyene diamictites might reflect a fourth Palaeoproterozoic glacial event unrecognized in North America, because the rise of atmospheric oxygen was recorded in the Timeball Hill Formation in South Africa (Bekker et al., 2004), but not in the post-Gowganda strata in the Huronian Supergroup in North America (Bekker et al., 2001). The latter interpretation, however, is not supported due to the following reasons: (i) geochronologic constraints for the glacial diamictites in Michigan and Wisconsin bracket the Gowganda Formation between 2288 ± 15 and 2131 ± 13 Ma (Fig. 1A, B), which is coeval to or slightly younger than the age bracket from 2316 ± 7 Ma to 2248.9 ± 5.9 Ma constrained for the lower Timeball Hill Formation (Hannah et al., 2004); (ii) no mature quartzite has been recognized below the Timeball Hill and Makganyene glacial diamictites, suggesting that the diamictites occurred at the bottom or in the lower portion of a sedimentary sequence, instead of in the upper portion or at the top; (iii) neither Makganyene Formation diamictites nor the upper part of the Timeball Hill Formation show any relationship with cap carbonates or banded iron formations (Bekker et al., 2005; Eriksson et al., 2011); (iv) there is no chronological evidence to support the fourth discrete Palaeoproterozoic glaciation episode; and (v) there is a ca. 70 Ma break between the deltaic deposits of the Timeball Hill and Boshoek formations and the overlying subaerial volcanic rocks of the Hekpoort Formation (Hannah et al., 2004). Thus, we prefer the interpretation that the Boshoek and Makganyene glacial diamictites are correlated with glacial diamictites in the Huronian Supergroup of North America. Similarly, the Meteorite Bore Member glacial diamictites of the Turee Creek Group in the Hamersley Basin, Western Australia should be correlated with the glacial diamictites in the Huronian Supergroup. The Duitschland glacial diamictites (>2424 Ma) might reflect another earlier glaciation event, which probably occurred at a high latitude or high altitude area and should be excluded from the records of the HGE, although it could be a prelude of the HGE.

Given that the HGE was globally synchronous, its timing can be constrained more accurately as shown in Fig. 2. As isotope dating of minerals and rocks from the diamictite units cannot determine

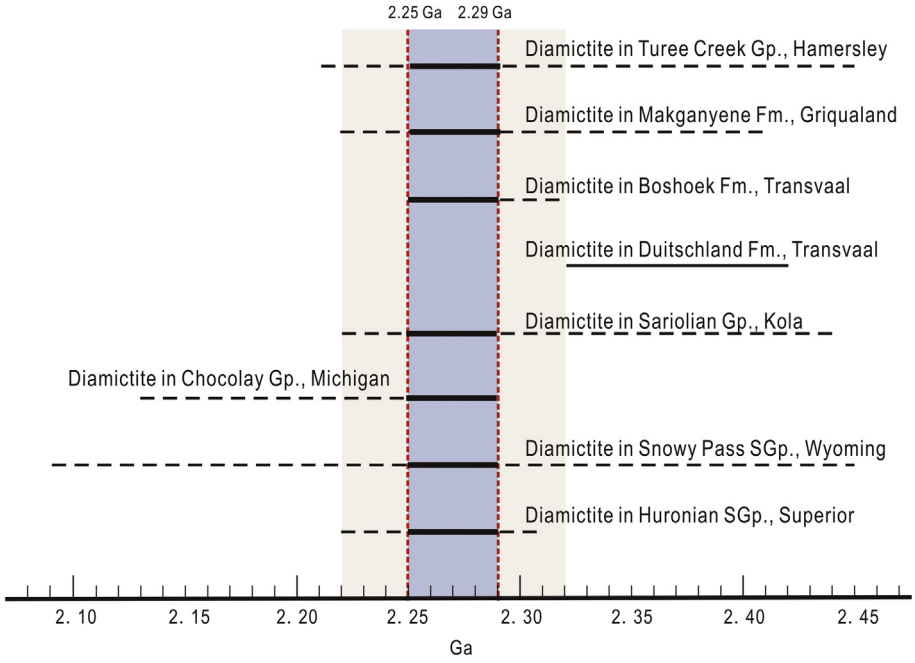

Figure 2. Sketches showing the timing of the global Palaeoproterozoic glaciation records.

their deposition time, the ages of diamictite units are mainly constrained in time ranges by using the ages of underlying and overlying volcanic rocks, or the ages of intrusions covered by or crosscutting the diamictite units (see Table 2 and discussion in Section 2). This means that the real duration of the glaciation is shorter or narrower, but within the ranges shown in Table 2 and Fig. 2. Hence, we can constrain the duration time of the HGE to be 2.32–2.22 Ga, and more concisely, to be 2.29–2.25 Ga.

4. Causes of the Huronian Glaciation Event

Models advanced to explain the onset of the Palaeoproterozoic global Huronian Glaciation Event include: (i) drawdown of atmospheric CO_2 as a result of increasing weathering caused by accretion and collision tectonics (Young, 1991); (ii) lowering CO_2 concentrations due to enhanced weathering of silicates caused by rifting of supercontinents at low latitudes (Evans et al., 1997; Evans, 2003); and (iii) greenhouse effect resulted from CH_4 elimination and atmospheric oxygenation (Pavlov et al., 2000; Kasting, 2004, 2005; Kopp et al., 2005).

4.1. Drawdown of atmospheric CO_2

The CO_2 percentage in atmosphere may have changed dramatically during the periods of intensive chemical weathering during Palaeoproterozoic times. Young (1991) indicated that the widespread 2.4–2.2 Ga glaciations might have been caused by decreasing amounts of greenhouse gases pumped into the atmosphere during waning of the superplume event, negative feedback of continental weathering, and ceasing albedo resulting from the formation of Neoarchaean supercontinent.

The terrestrial CO_2 budget is balanced between sources and sinks. The sources include the deep ocean, decomposed organic matter, and volcanic and metamorphic degassing; and the sinks are the ocean surface, atmosphere and organic debris (Sundquist, 1993; Melezhik, 2006), as well as the carbonate sedimentation and crust surface carbonation (Tang et al., 2004). During active rifting, outgassing of CO_2 related to voluminous continental volcanism may have been sufficient to balance the predicted large CO_2 drawdown by chemical weathering. High atmospheric CO_2 percentage prevented cooling and was suggested to be a major factor in the lack of Archaean glaciations, which might also reflect a lack of large Archaean continents.

As documented in Fennoscandian Shield, palaeotopography was defined by large rift-separated uplifts and the weathering as well as deep erosion (down to 2–3 km) of the Archaean crust (Melezhik, 2006). Such processes should have inevitably resulted in an enhanced silicate weathering rate and a considerable consumption of atmospheric CO_2. Similarly, other Huronian glacial diamictites from North America and South Africa are developed above angular unconformities, suggesting that erosion of flood-basalts might have provided an enhanced flux of materials to the ocean on a

Table 2
Reassessment of the ages of the Palaeoproterozoic glaciogenic diamictites in the world.

Area	Diamictite-bearing strata	Maximum age	Minimum age
Superior, Canada	Hough Lake, Quirke Lake & Cobalt Gps., Huronian SGp.	2.33 Ga	2.22 Ga
Wyoming, USA	Deep Lake & Lower Libby Creek Gps., Snowy Pass SGp.	<2.45 Ga	>2.09 Ga
Michigan, USA	Enchantment Lake Fm., Chocolay Gp.	2.29 Ga	2.13 Ga
Kola, Fennoscandian, Russia	Polisarska Fm., Sariolian Gp.	2.44 Ga	2.22 Ga
Transvaal, S Africa	Duitschland Formation, Pretoria Gp.	2.42 Ga	2.32 Ga
Transvaal, S Africa	Boshoek Fm., Pretoria Gp., Transvaal SGp.	2.32 Ga	2.25 Ga
Griqualand West, S Africa	Makganyene Fm., Postmasburg Gp., Transvaal SGp.	2.41 Ga	2.22 Ga
Hamersley, W Australia	Meteorite Bore Mb., Kungarra Fm., Turee Creek Gp.	2.45 Ga	2.21 Ga

semiglobal scale (Bekker et al., 2005, 2006; Eriksson et al., 2011). Extraction of CO_2 from the atmosphere can be seen as related to extensive chemical weathering of Ca and Mg silicates and at the same time relative O_2 content could have increased dramatically (Raymo, 1991; Melezhik, 2006; Eriksson et al., 2011). The glacial eras themselves are noted for disturbances to the carbon cycle, as manifested by $\delta^{13}C$ (Bekker and Kaufman, 2007).

Atmospheric CO_2 drawdown would have been enhanced by large-scale fresh basaltic surfaces which should create particularly strong CO_2 sinks (Taylor and Lasaga, 1999; Dessert et al., 2001). It has been demonstrated that the considerable consumption of atmospheric CO_2 by fresh basaltic surfaces severely impacted the global climate during younger periods and led to global refrigeration lasting over a million of years (Dessert et al., 2001, 2003).

This model can be supported by geological data as the following: (i) basalts or mafic rocks were widely developed in Archaean or pre-Huronian granite-greenstone terrains; (ii) in several areas, such as the Superior Craton and Pilbara Block (i.e., Fortescue Group; Taylor and McLennan, 1985), flood basalts can be observed underlying the Huronian diamictite units; and (iii) carbonate strata developed before the HGE, such as the Wittenoom Formation of Hamersley Group and Kungarra Formation of Turee Creek Group in West Australia; and the Chuniespoort Group and the Duitschland Formation of the Lower Pretoria Group in Transvaal Basin, South Africa. Despite of this, the CO_2 drawdown model disagrees with the following facts: (i) as shown in Fig. 1, the basalts overlying the Huronian diamictites are far more than those underlying the diamictites, but did not followed with glacial records; (ii) the post-Huronian carbonates are more widespread than the pre-Huronian carbonates; and (iii) the black shales which are abundant in organic debris overlie, rather than underlie, the Huronian glaciogenic diamictite units (Fig. 1C).

4.2. Latitude-related glaciation

According to Eyles (2008) and Eriksson et al. (2011), common factors in the glaciations are major supercontinental fragmentation and reassembly events, along with climate perturbations most likely related to weathering induced drawdown of CO_2 at low latitudes.

Assuming that the pre-Huronian major landmasses were in low-latitude position, the CO_2 consumption via silicate weathering can be in the order of five magnitudes higher as compared to other climatic regions (Dessert et al., 2003). Carbon isotope values of pre-Huronian carbonates (Bekker et al., 2003a) indicate that the recycling of the organic matter was not effective, resulting in reduced CO_2 emissions. This would have amplified the decline of atmospheric CO_2, which was already in decline from drawdown due to enhanced silicate weathering in low-latitude positions. Hence, net CO_2 emission was significantly reduced while the sink was drastically increased. This would have led to the considerable drawdown of atmospheric CO_2 and the onset of global cooling and, ultimately, to glacial conditions (Melezhik, 2006).

Although orography and ocean circulation in relation to high-latitude continents influences the occurrence and intensity of glaciation, model results clearly show that widespread glaciations interrupting warmer climate must be associated with periods of low atmospheric $p(CO_2)$, thus making the linkage to the global geochemical cycles of oxygen and carbon (Fairchild and Kennedy, 2007).

There are no direct data suggesting palaeogeographic locations of the glacial deposits, but the large continental flood-basalt provinces in Australia (Barley et al., 1997), Fennoscandia (Puchtel et al., 1996, 1997; Heaman, 1997), North America (Heaman, 1997; Vogel et al., 1998) and possibly in India (Bhat et al., 1998) were erupted in regionally uplifted and rifted continents in low-latitude positions at ca. 2450 Ma, immediately prior to the onset of the glaciation. In a palaeolatitudinal drift construction for Fennoscandia drawn up by Mertanen et al. (1989), the Karelian Craton drifted from high to moderate latitudes with no major rotations during Palaeoproterozoic times. Whereas the Karelian Craton shifted to lower latitudes, the adjacent North American Craton might have moved to a position to undergo further glaciations at high latitudes. Palaeomagnetic studies indicate a near-equatorial palaeolatitude for the Ongeluk lava (De Kock et al., 2009b) and hence for the near-contemporaneous Makganyene diamictite (Evans et al., 1997).

However, the latitude-related glaciation model cannot explain the occurrence of several successive glaciations on the same craton, as is recorded in the Huronian Supergroup (Strand, 2012) and Snowy Pass Supergroup, as well as Transvaal Basin. Therefore, the glaciations may have fluctuated, not only with orbital but also with atmospheric changes (Young, 1991; Young et al., 2001).

4.3. Elimination of CH_4

Early Earth's atmosphere was apparently dominated by CH_4 which was responsible for a warm climate (e.g., Chen, 1990, 1996; Pavlov et al., 2000). Removal of most of the CH_4 by oxidation due to the rise of O_2 at 2320 Ma (Farquhar et al., 2000; Pavlov and Kasting, 2002; Bekker et al., 2004; Frei et al., 2009; Konhauser et al., 2009) has been considered as a cause of the Palaeoproterozoic glaciation(s) (Pavlov et al., 2000; Kasting, 2004, 2005) and even for the onset of the Palaeoproterozoic Snowball Earth (Kopp et al., 2005).

However, the CH_4-centred model cannot explain how the Earth recovered from the global glaciation, and why it did not experience new glaciations in the following 1500 Ma time interval. Thus, other greenhouse gases such as CO_2 and water vapour could have played an equally important role (Bekker and Kaufman, 2007). The only way of removing CO_2 as well as oxidized CH_4 from the atmosphere is either by biological photosynthesis or via a carbonate-silicate geochemical cycle.

The Palaeoproterozoic glacial epoch has been related to the transition from the anoxic CH_4-rich atmosphere to an oxic, CO_2-rich atmosphere (e.g., Chen, 1996; Pavlov et al., 2000; Claire et al., 2006; Goldblatt et al., 2006); and the multiplicity of ice ages is arguably related to oscillations in O_2 and CH_4 as well as CO_2 production. Bekker et al. (2005) speculated that fluctuating atmospheric oxygen level during the Palaeoproterozoic glacial epoch led to a stepwise increase in atmospheric CO_2 contents at the expense of methane. ^{13}C depleted organic matter (e.g., Pecors Formation; Fig. 1B) formed in the aftermath of the oldest Palaeoproterozoic glacial epoch provides the convincing evidence for biogeochemical methane cycling above the wave base in the Huronian Basin (Bekker and Kaufman, 2007). Some methane produced below the redox boundary escaped to the atmosphere and the consequent balance between biogeochemical methane and oxygen production modulated climatic changes during the Palaeoproterozoic glacial epoch.

The Palaeoproterozoic HGE was shortly followed by one or more remarkable positive $\delta^{13}C_{carb}$ excursions variously termed as the Lomagundi Event (Schidlowski et al., 1975, 1976; Bekker et al., 2006; Tang et al., 2011; and references therein), the Jatulian Event (Melezhik et al., 1999b) or the Great Oxidation Event (GOE) (Karhu and Holland, 1996; Anbar et al., 2007; Konhauser et al., 2009; Zhao, 2010). The release of oxygen during this profound biogeochemical anomaly would have conspicuously decreased atmospheric methane levels before atmospheric CO_2 fell below the level required to maintain greenhouse conditions alone. This event most likely marked the irreversible transition to an oxygenated

atmosphere with a nearly constant percentage of CO_2 thereafter acting as the major greenhouse gas throughout the rest of Earth's history.

4.4. BIF deposition: a new model

Increasing icehouse gases such as O_2 and decreasing greenhouse gases such as CH_4 and CO_2 will inevitably cool the hydrosphere-atmosphere system and resulted in glaciation event. However, a reducing hydrosphere-atmosphere system prevented from oxygenation, because the O_2 generated from biological photosynthesis must be instantly consumed in oxidation of the reducing components accumulated in an anoxic system. Therefore, removal or drawdown of reducing components from the system is the prerequisite for a glaciation event.

The early Earth's hydrosphere-atmosphere system was obviously anoxic from ~4.5 to 2.5 Ga (Cloud, 1968, 1973; Holland, 1994; Rye and Holland, 1998). Such a long anoxic history made the Archaean hydrosphere enriched with a large amount of low-valent ions represented by Fe^{2+}. Since the beginning of the Palaeoproterozoic era, biological photosynthesis was enhanced (Melezhik et al., 1997a, 1999a; Chen et al., 2000), which transferred CO_2 into organic debris and O_2; the O_2 was consumed in oxidation of the accumulated Fe^{2+} and CH_4 in the ways of $4Fe^{2+} + O_2 + 10H_2O = 4Fe(OH)_3 + 8H^+$, and $CH_4 + 2O_2 = CO_2 + 2H_2O$. During these processes, O_2 was generated, atmospheric CO_2 drawdown occurred, CH_4 was eliminated, BIF was deposited, and the CO_2 in hydrosphere-atmosphere system was relatively enriched in ^{13}C due to the fixation of ^{12}C in organic debris (Schidlowski et al., 1975; Schidlowski, 1988). After removal of the majority of reducing components from the oceans which is indicated by widespread deposition of BIFs (Bekker et al., 2010; Zhai and Santosh, 2013), the O_2 produced by biological photosynthesis gradually began to accumulate in atmosphere and resulted in HGE due to the icehouse effect of O_2.

The above interpretation is consistent with the scenario shown in Fig. 1, in particularly, the worldwide development of voluminous BIFs in the period of 2.5–2.3 Ga which is termed as the Siderian.

5. Linkage between the GOE and HGE

The tectonic processes and global environmental changes during the Palaeoproterozoic (2.5–1.6 Ga) have been the focus of numerous studies in the past decades. Schidlowski et al. (1975, 1976) firstly reported the positive $\delta^{13}C_{carb}$ anomaly in the Palaeoproterozoic carbonates from Karelia (Russia) and the Fennoscandian Shields, as well as in the dolomites with ages of 2.65–1.95 Ga from the Lomagundi Province (Zimbabwe) where the $\delta^{13}C_{carb}$ values are even up to 12‰. They also related this phenomenon to the oxidation of the atmosphere. However, this important discovery had been largely neglected for a long time.

In 1989, the International Commission on Stratigraphy recommended 2.3 Ga to be a defining boundary in the Precambrian Stratigraphy Chart. Thereafter positive $\delta^{13}C_{carb}$ excursions have been recognized worldwide in 2.33–2.06 Ga carbonate rocks (Schidlowski, 1988; Strauss et al., 1992; Karhu, 1993; Karhu and Holland, 1996; Melezhik et al., 1999b; Bekker et al., 2003a,b; Bekker et al., 2006; Tang et al., 2011, 2013 and references therein). Karhu and Holland (1996) reassessed new data for the carbon isotopic composition of carbonates and paired carbonates–total organic carbon (TOC) deposited in Palaeoproterozoic, and revealed the very large positive $\delta^{13}C_{carb}$ excursion during 2.22–2.06 Ga. They related the positive $\delta^{13}C_{carb}$ excursion to a rapid organic carbon deposition which had been globally recognized as an extensive accumulation of organic matter (Strauss et al., 1992; Melezhik et al., 1997a, 1999a; Chen et al., 2000; Lai et al., 2012), and estimated that the associated total excess O_2 produced was up to 12–22 times as compared to the present atmospheric O_2 inventory. Consequently, the Palaeoproterozoic worldwide positive $\delta^{13}C_{carb}$ excursion was suggested as an indicator of the Great Oxidation Event (GOE) of the atmosphere (Karhu and Holland, 1996). Genetically, the GOE was related to the breakup of the Kenorland/Superia supercontinent (Bekker and Eriksson, 2003), and to a 2.3 Ga environmental catastrophe indicated by the contrasting REE geochemical signatures between pre- and post-2.3 Ga sediments (Chen, 1988; Chen and Zhao, 1997; Chen et al., 2000; Tang et al., 2012).

The timing and extent of early Earth oxygenation are highly controversial and have been the topics of numerous studies (Canfield et al., 2000; Kasting, 2001; Canfield, 2005). It is accepted that the atmosphere and hydrosphere was reducing before 2.45 Ga, followed by a rapid rise in $p(O_2)$ from $<10^{-5}$ times the present atmospheric level (PAL) at some time between ~2.3 and 1.8 Ga (Cloud, 1968, 1973; Holland, 1994, 2002; Rye and Holland, 1998; Kasting and Siefert, 2002). Some indicators (e.g., oxidation state of palaeosols, occurrence of uranium, and the appearance of red beds) showed that the level of oxygen in the atmosphere rose between 2.22 and 2.06 Ga from $<2 \times 10^{-3}$ atm (1% of PAL) to >0.03 atm (15% of PAL) (Holland, 1994).

The classic and long-standing model of the 2.3 Ga GOE is debated in recent studies. Bekker et al. (2004) argued that the rise of atmospheric oxygen had occurred by 2.32 Ga. They found that the sulphur isotopic composition of the syngenetic pyrite from the 2.32 Ga organic-rich shales of (Hannah et al., 2004) Rooihoogte and Timeball Hill formations, South Africa (Fig. 1E), has a wide range and shows no evidence of mass-independent fractionation. This indicates that atmospheric oxygen was present at a significant level ($>10^{-5}$ times the PAL) during the deposition of those units. The presence of rounded pebbles of sideritic iron formation at the base of the Rooihoogte Formation and an extensive and thick ironstone layer consisting of haematitic pisolites and oölites in the upper Timeball Hill Formation also indicate that atmospheric oxygen rose significantly. These units were suggested to have deposited between the second and third of the three Palaeoproterozoic glacial events (Fig. 1E). Enrichment of the redox-sensitive transition metals, such as Mo and Re, in the late Archaean Mount McRae Shale in Western Australia (Fig. 1G), together with S-isotope signature, indicates "a whiff of oxygen" occurred >50 Ma prior to the 2.45–2.32 Ga GOE (Anbar et al., 2007; Kaufman et al., 2007). Wille et al. (2007) reported rapid fluctuation of Mo isotopic values in the 2.64–2.5 Ga black shales of the Ghaap Group (Transvaal Supergroup) and suggested that the ocean at that time frequently recurred oxygen-free conditions alternated with cyanobacterial production of oxygen. However, Mo isotopic data from the Ghaap Group carbonate rocks show an opposite trend of constancy and support a near-continuous presence of oxygen, though at lower levels than in the black shales (Voegelin et al., 2010). The fluctuation of Mo isotopes in the black shales may rather reflect detrital inputs and concomitant dilution effects, or redox changes in the depositional environment, or both, and thereby stressing the basin-scale environmental influences (Voegelin et al., 2010). Cr isotope changes (another oxygen proxy) from 2.8 to 2.6 Ga BIF indicate a transient rise in atmospheric and oceanic oxygen, prior to the GOE of 2.45–2.2 Ga (Frei et al., 2009). Eriksson et al. (2009, 2011) argued that the global change in oxygen levels during 2.4–1.8 Ga is rather a diachronous than the simple panacea of a universally applied 2.3 Ga GOE.

Both the positive $\delta^{13}C_{carb}$ excursion and the GOE couched at the Huronian glaciation period. As shown in Fig. 1, all the

Palaeoproteozoic carbonate rocks with positive $\delta^{13}C_{carb}$ anomaly (Tang et al., 2011, 2013; and references therein) overlie the glacial diamictites; whilst the carbonates sandwiched between the second and third glacial deposits show negative $\delta^{13}C_{carb}$ ratios, e.g., the Espanola Formation in southern Ontario (Fig. 1B) and the Vagner Formation in Wyoming (Fig. 1C), and are considered as cap carbonates (Bekker et al., 2003a, 2005). Young (2012a) argued that the Espanola Formation was probably formed as a result of ponding and evaporation in a hydrothermally influenced, restricted rift setting, and listed evidences as the following: (i) the Espanola Formation is more thicker (ca. 150–600 m) than Neoproterozoic cap carbonates; (ii) it has a complex stratigraphy and sedimentary structures and exhibits considerable lateral variability (Bernstein and Young, 1990); (iii) intimate association of carbonates with fine-grained siliciclastic rocks (siltstones) in the Espanola Formation is differing from the Neoproterozoic cap carbonates which rapidly deposited during post-glacial sea-level rise that precluded the introduction of siliciclastic materials (Hoffman et al., 1998); and (iv) the strong ^{18}O-depletion in the Espanola Formation carbonates is consistent with pervasive carbonate recrystallization, element remobilization, and/or possible hydrothermal alteration (Bekker et al., 2005; Tang et al., 2013).

Though the timing of atmospheric $p(O_2)$ up to 10^{-5} times of the PAL was proposed as between the second and third of the three-episodic Huronian Glaciation Event (Bekker et al., 2004), even >50 Ma prior to the 2.45–2.32 Ga (Anbar et al., 2007; Kaufman et al., 2007) or prior to the first Palaeoproterozoic glacial episode (Wille et al., 2007; Voegelin et al., 2010; Czaja et al., 2012), the partisan sedimentary evidence supporting the GOE is the world-wide development of "red beds" (Melezhik et al., 1999b), overlapped with the positive $\delta^{13}C_{carb}$ excursion. The Palaeoproterozoic red beds have been recognized in the Cobalt Group and its equivalents in North America (Young et al., 2001), the Upper Jatulian Group in Fennoscandian (Melezhik et al., 1997a), The Pretoria Group and Waterberg Group in South Africa (Eriksson and Cheney, 1992; Eriksson et al., 2011) and other cratons in the world (Chen, 1996). Within the Pretoria Group, the iron colouration is restricted to matrix material, while in the Waterberg Group, grain surfaces are stained partially red by iron oxides (Eriksson et al., 2011).

Integrating the data and interpretations, we consider that the Huronian Glaciation Event, the positive $\delta^{13}C_{carb}$ excursion, and the appearance of red beds are significant events that occurred in younging order with somewhat temporal overlap. These events, together with other Earth's superficial changes, resulted from, or relate to, the GOE which should have commenced earlier than the HGE, i.e., before 2.3 Ga, and recorded global changes in the atmosphere, biosphere, hydrosphere and lithosphere. However, the beginning of the GOE has not been well constrained. Here we propose a two-stage oxygenation model, i.e., the oxidation of the hydrosphere during 2.5–2.3 Ga and then the oxygenation of the atmosphere during 2.3–2.2 Ga (Fig. 3).

The Archaean hydrosphere-atmosphere system was well accepted to be anoxic, although there was minor oxygen resulted from possibly local biological photosynthesis as revealed by the studies of S, Mo, Fe and Cr isotopes (Anbar et al., 2007; Kaufman et al., 2007; Wille et al., 2007; Frei et al., 2009; Voegelin et al., 2010; Czaja et al., 2012). In reducing hydrosphere, the dissolved elements (anions or cations) must be present as low valences. For examples, the Fe, Eu, Mo, Cr and S will be dominated by Fe^{2+}, Eu^{2+}, Mo^{4+}, Cr^{2+} and S^{2-}, respectively, rather than by Fe^{3+}, Eu^{3+}, Mo^{6+}, Cr^{6+} and S^{6+} that stably exist in oxidizing environment. It can be envisaged that a huge quantity of low-valent cations and anions were accumulated in the hydrosphere during a 2 Ga-long (from ~4.5 to 2.5 Ga) reducing Earth's evolution. In early stage of the GOE, i.e., 2.5–2.3 Ga, oxygen generated from biological photosynthesis should be instantly consumed during oxidation of the accumulated low-valent components, resulting in precipitation as typically represented by banded iron formations (Fig. 3). After the oxidation of the majority of the low-valent ions in the oceans, the O_2 produced by biological photosynthesis gradually accumulated in the atmosphere at expense of CO_2, i.e., atmospheric oxygenation (Fig. 3). Along with increasing O_2 in atmosphere, drawdown of CO_2 and elimination of CH_4, the icehouse effect of O_2 cooled the climate and resulted in the 2.29–2.25 Ga HGE, followed by widespread deposition of carbonates with positive $\delta^{13}C_{carb}$ anomalies and red beds during 2.25–2.06 Ga (Fig. 3). Therefore, we suggest that the GOE mainly occurred in the period of 2.5–2.2 Ga, including the earlier hydrosphere oxidation stage and later atmosphere oxygenation stage.

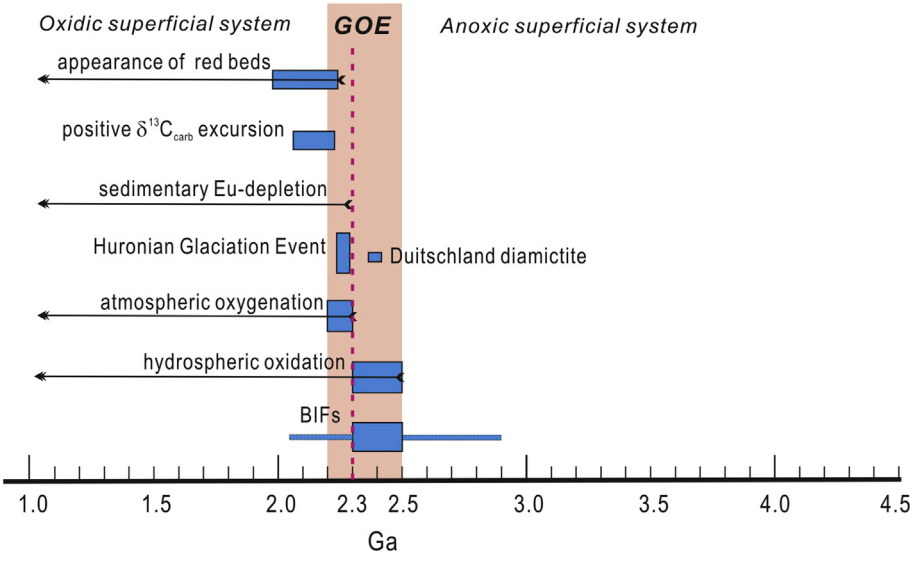

Figure 3. A summary chart of the environmental changes at ca. 2.3 Ga.

6. Concluding remarks

Palaeoproterozoic glaciogenic diamictite units have been recognized in the major continents of the world and can be distinguished between the earlier, locally-developed, pre-2.3 Ga Duitschland glacial diamictites in South Africa and the globally-developed, 2.32–2.22 Ga (more concisely, 2.29–2.25 Ga) Huronian Glaciation Event.

The global Huronian Glaciation Event slightly postdated the widespread deposition of the Siderian banded iron formations, followed by the development of the carbonate strata with positive $\delta^{13}C_{carb}$ anomalies and the oldest red beds in each continents, should be associated with, or could be a result of, the global Great Oxidation Event. The GOE includes the early-stage hydrosphere oxidation (2.5–2.3 Ga) and the late-stage atmospheric oxygenation (2.3–2.2 Ga).

A pre-2.3 Ga reducing hydrosphere prevented atmosphere from oxygenation, because of the consumption of O_2 generated from biological photosynthesis in the oxidation of Fe^{2+} and precipitation of BIFs. After 2.3 Ga, increasing O_2 and decreasing CH_4 and CO_2 cooled the hydrosphere-atmosphere system and resulted in the global Huronian Glaciation Event. Therefore, removal or drawdown of reducing components from the system is the prerequisite for a glaciation event.

Acknowledgements

This study was funded by the National 973-Program (Project Nos. 2012CB416602, 2006CB403508) and National Natural Science Foundation of China (Nos. 40352003, 40425006, 40373007) and Frontier Field Project of the State Key Laboratory of Ore Deposit Geochemistry, Institute of Geochemistry, Chinese Academy of Sciences. We thank Dr. Yong-Fei Yang and Xiao-Hua Deng of the Peking University for their valuable discussions. We are grateful to Prof. S. Mohanty for his invitation to submit this paper. Constructive suggestions, pertinent comments and careful corrections by anonymous reviewer and Prof. M. Santosh greatly improved the quality of the manuscript.

References

Altermann, W., Nelson, D.R., 1998. Sedimentation rates, basin analysis and regional correlations of three Neoarchaean and Palaeoproterozoic sub-basins of the Kaapvaal craton as inferred from precise U–Pb zircon ages from volcaniclastic sediments. Sedimentary Geology 120, 225–256.

Amelin, Yu.V., Heaman, L.M., Semenov, V.S., 1995. U–Pb geochronology of layered mafic intrusions in the eastern Baltic Shield: implications for the timing and duration of Palaeoproterozoic continental rifting. Precambrian Research 75, 31–46.

Anbar, A.D., Duan, Y., Lyons, T.W., Arnold, G.L., Kendall, B., Creaser, R.A., Kaufman, A.J., Gordon, G.W., Scott, C., Garvin, J., Buick, R., 2007. A whiff of oxygen before the great oxidation event? Science 317, 1903–1906.

Andrews, A.J., Masliwec, A., Morris, W.A., Owsiacki, L., York, D., 1986. The silver deposits at Cobalt and Gowganda, Ontario. II: an experiment in age determinations employing radiometric and paleomagnetic measurements. Canadian Journal of Earth Sciences 23, 1507–1518.

Argast, A., 2002. The lower Proterozoic Fern Creek Formation, northern Michigan: mineral and bulk geochemical evidence for its glaciogenic origin. Canadian Journal of Earth Sciences 39, 481–492.

Aspler, L.B., Chiarenzelli, J.R., 1998. Two Neoarchean supercontinents? Evidence from the Paleoproterozoic. Sedimentary Geology 120, 75–104.

Babinski, M., Chemale Jr., F., Van Schmus, W.R., 1995. The Pb/Pb age of the Minas Supergroup carbonate rocks, Quadrilátero Ferrífero, Brazil. Precambrian Research 72, 235–245.

Balashov, Yu.A., Fedotov, Zh.A., Skufin, P.K., 1994. Rb–Sr dating of the lower volcanogenic series in the Pechenga complex, the Kola Peninsula. Geochemistry International 31, 85–90.

Barley, M.E., Pickard, A.L., Sylvester, P.L., 1997. Emplacement of a large igneous province as a possible cause of banded iron formation 2.45 billion years ago. Nature 385, 55–58.

Bau, M., Romer, R.L., Lüders, V., Beukes, N.J., 1999. Pb, O, and C isotopes in silicified Mooidraai dolomite (Transvaal Supergroup, South Africa): implications for the composition of Paleoproterozoic seawater and 'dating' the increase of oxygen in the Precambrian atmosphere. Earth and Planetary Science Letters 174, 43–57.

Bekker, A., Eriksson, K.A., 2003. A Paleoproterozoic drowned carbonate platform on the southeastern margin of the Wyoming Craton: a record of the Kenorland breakup. Precambrian Research 120, 327–364.

Bekker, A., Holland, H.D., Wang, P.L., Rumble, D., Stein, H.J., Hannah, J.L., Coetzee, L.L., Beukes, N.J., 2004. Dating the rise of atmospheric oxygen. Nature 427, 117–120.

Bekker, A., Karhu, J.A., Kaufman, A.J., 2006. Carbon isotope record for the onset of the Lomagundi carbon isotope excursion in the Great Lakes area, North America. Precambrian Research 148, 145–180.

Bekker, A., Kaufman, A.J., 2007. Oxidative forcing of global climate change: a biogeochemical record across the oldest Paleoproterozoic ice age in North America. Earth and Planetary Science Letters 258, 486–499.

Bekker, A., Kaufman, A.J., Karhu, J.A., Beukes, N.J., Swart, Q.D., Coetzee, L.L., Eriksson, K.A., 2001. Chemostratigraphy of the Paleoproterozoic Duitschland Formation, South Africa: implications for coupled climate change and carbon cycling. American Journal of Science 301, 261–285.

Bekker, A., Kaufman, A.J., Karhu, J.A., Eriksson, K.A., 2005. Evidence for Paleoproterozoic cap carbonates in North America. Precambrian Research 137, 167–206.

Bekker, A., Karhu, J.A., Eriksson, K.A., Kaufman, A.J., 2003a. Chemostratigraphy of Palaeoproterozoic carbonate successions of the Wyoming Craton: tectonic forcing of biogeochemical change? Precambrian Research 120, 279–325.

Bekker, A., Sial, A.N., Karhu, J.A., Ferrerira, V.P., Noce, C.M., Kaufman, A.J., Romano, A.W., Pimentel, M.M., 2003b. Chemostratigraphy of carbonates from the Minas Supergroup, Quadrilátero Ferrífero (Iron Quadr-angle), Brazil: a stratigraphic record of early Proterozoic atmospheric, biogeochemical and climatic change. American Journal of Science 303, 865–904.

Bekker, A., Slack, J.F., Planavsky, N., Krapež, B., Hofmann, A., Konhauser, K.O., Rouxel, O.J., 2010. Iron formation: the sedimentary product of a complex interplay among mantle, tectonic, oceanic, and biospheric processes. Economic Geology 105, 467–508.

Bernstein, L., Young, G.M., 1990. Depositional environments of the Early Proterozoic Espanola Formation. Canadian Journal of Earth Sciences 27, 539–551.

Beukes, N.J., 1986. The Transvaal sequence in Griqualand west. In: Anhaeusser, C.A.R., Maske, S. (Eds.), Mineral Deposits of Southern Africa, vol. 1. Geological Society of South Africa, Johannesburg, pp. 819–828.

Bhat, M.I., Claesson, S., Dubey, A.K., Pande, K., 1998. Sm–Nd age of the Garhwal–Bhowali volcanics, western Himalayas: vestiges of the late Archaean Rampur flood basalt province of the northern Indian craton. Precambrian Research 87, 217–231.

Blake, T.S., Barley, M.E., 1992. Tectonic evolution of the late Archaean to early Proterozoic Mount Bruce Megasequence Set, western Australia. Tectonics 11, 1415–1425.

Bleeker, W., 2003. The late Archean record: a puzzle in ca. 35 pieces. Lithos 71, 99–134.

Buick, I.S., Maas, R., Gibson, R., 2001. Precise U–Pb titanite age constraints on the emplacement of the Bushveld Complex, South Africa. Journal of the Geological Society of London 158, 3–6.

Buick, I.S., Uken, R., Gibson, R.L., Wallmach, T., 1998. High-$\delta^{13}C$ Paleoproterozoic carbonates from the Transvaal Supergroup, South Africa. Geology 26, 875–878.

Button, A., 1986. The Transvaal sub-basin of the Transvaal Sequence. In: Anhaeusser, C.R., Maske, S. (Eds.), Mineral Deposits of Southern Africa, vol. 1. Geological Society of South Africa, Johannesburg, pp. 811–817.

Canfield, D.E., 2005. The early history of atmospheric oxygen: homage to Robert M. Garrels. Annual Review of Earth and Planetary Sciences 33, 1–36.

Canfield, D.E., Habicht, K.S., Thamdrup, B., 2000. The Archean sulfur cycle and the early history of atmospheric oxygen. Science 288, 658–661.

Chandler, F.W., 1984. Sedimentary setting of an Early Proterozoic copper occurrence in the Cobalt Group, Ontario: a preliminary assessment. Current Research, Part A. Geological Survey of Canada, 185–192. Paper 84–1A.

Chandler, F.W., 1988. Diagenesis of sabkha-related, sulphate nodules in the early Proterozoic Gordon Lake Formation, Ontario, Canada. Carbonates and Evaporites 3, 75–94.

Chemale Jr., F., Rosie`re, C.A., Endo, I., 1994. The tectonic evolution of the Quadrilátero Ferrífero, Minais Gerais, Brazil. Precambrian Research 65, 25–54.

Chen, Y.J., 1988. Catastrophe of the geologic environment at 2300 Ma. In: Abstracts of International Symposium on Geochemistry and Mineralization of Proterozoic Mobile Belts, Tianjin, September 6–10, pp. 11.

Chen, Y.J., 1990. Evidences for the catastrophe in geologic environment at about 2300 Ma and the discussions on several problems. Journal of Stratigraphy 14, 178–186 (in Chinese with English abstract).

Chen, Y.J., 1996. Progresses in application of sedimentary trace element geochemistry to probe crustal composition and environmental change. Geology Geochemistry (3), 1–125 (in Chinese).

Chen, Y.J., Su, S.G., 1998. Catastrophe in geological environment at 2300 Ma. Mineralogical Magazine 62A (1), 320–321.

Chen, Y.J., Liu, C.Q., Chen, H.Y., Zhang, Z.J., Li, C., 2000. Carbon isotope geochemistry of graphite deposits and ore-bearing khondalite series in North China: implications for several geoscientific problems. Acta Petrologica Sinica 16, 233–244 (in Chinese with English abstract).

Chen, Y.J., Zhao, Y.C., 1997. Geochemical characteristics and evolution of REE in the Early Precambrian sediments: evidences from the southern margin of the North China Craton. Episodes 20, 109–116.

Cheney, E.S., 1996. Sequence stratigraphy and plate tectonic significance of the Transvaal succession of southern Africa and its equivalent in Western Australia. Precambrian Research 79, 3–24.
Claire, M.W., Catling, D.C., Zahnle, K.J., 2006. Biogeochemical modelling of the rise in atmospheric oxygen. Geobiology 4, 239–269.
Cloud, P.E., 1968. Atmospheric and hydrospheric evolution on the primitive earth. Science 160, 729–736.
Cloud, P.E., 1973. Paleoecological significance of banded iron-formation. Economic Geology 68, 1135–1143.
Cornell, D.H., Schütte, S.S., Eglington, B.L., 1996. The Ongeluk basaltic andesite formation in Griqualand West, South Africa: submarine alteration in a 2222 Ma Proterozoic sea. Precambrian Research 79, 101–123.
Cox, D.M., Frost, C.D., Chamberlain, K.R., 2000. 2.01-Ga Kennedy dike swarm, southeastern Wyoming: record of a rifted margin along the southern Wyoming province. Rocky Mountain Geology 35 (1), 7–30.
Czaja, A.D., Johnson, C.M., Roden, E.E., Beard, B.L., Voegelin, A.R., Nägler, T.F., Beukes, N.J., Wille, M., 2012. Evidence for free oxygen in the Neoarchean ocean based on coupled iron–molybdenum isotope fractionation. Geochimica et Cosmochimica Acta 86, 118–137.
Dahl, P.S., Holm, D.K., Gardner, E.T., Hubacher, F.A., Foland, K.A., 1999. New constraints on the timing of Early Proterozoic tectonism in the Black Hills (South Dakota), with implications for docking of the Wyoming province with Laurentia. Geological Society of America Bulletin 111, 1335–1349.
De Kock, M.O., Evans, D.A.D., Beukes, N.J., 2009a. Validating the existence of Vaalbara in the Neoarchean. Precambrian Research 174, 145–154.
De Kock, M.O., Evans, D.A.D., Kirschvink, J.L., Beukes, N.J., Rose, E., Hilburn, I., 2009b. Paleomagnetism of a Neoarchean–Paleoproterozoic carbonate ramp and carbonate platform succession (Transvaal Supergroup) from surface outcrop and drill core, Griqualand West region, South Africa (in Initial investigations of a Neoarchean shelf margin-basin transition (Transvaal Supergroup, South Africa)). Precambrian Research 169, 80–99.
Dessert, C., Dupré, B., François, L.M., Schott, J., Gaillardet, J., Chakrapani, G.J., Bajpai, S., 2001. Erosion of Deccan Traps determined by river geochemistry: impact on the global climate and $^{87}Sr/^{86}Sr$ ratio of seawater. Earth and Planetary Science Letters 188, 459–474.
Dessert, C., Dupré, B., Gaillardet, J., François, L.M., Allègre, C.J., 2003. Basalt weathering laws and the impact of basalt weathering on the global carbon cycle. Chemical Geology 202, 257–273.
Dorland, H.C., 2004. Provenance ages and timing of sedimentation of selected Neoarchean and Paleoproterozoic successions on the Kaapvaal Craton. Ph.D. Thesis. Rand Afrikaans University, Johannesburg, South Africa, 326 pp.
Endo, I., Hartmann, L.A., Suita, M.T.F., Santos, J.O.S., Frantz, J.C., McNaughton, N.J., Barley, M.E., Carneiro, M.A., 2002. Zircon SHRIMP isotopic evidence for Neoarchaean age of the Minas Supergroup, Quadrilátero Ferrífero, Minas Gerais. In: Congresso Brasileiro de Geologia. Sociedade Brasileira de Geologia, João Pessoa. Anais, 518.
Eriksson, P.G., Cheney, E.S., 1992. Evidence for the transition to an oxygen-rich atmosphere during the evolution of red beds in the Lower Proterozoic sequences of southern Africa. Precambrian Research 54, 257–269.
Eriksson, P.G., Lenhardt, N., Wright, D.T., Mazumder, R., Bumby, A.J., 2011. Late Neoarchaean–Palaeoproterozoic supracrustal basin-fills of the Kaapvaal craton: relevance of the supercontinent cycle, the “Great Oxidation Event” and “Snowball Earth”? Marine and Petroleum Geology 28, 1385–1401.
Eriksson, P.G., Rautenbach, CA.J.deW., Wright, D.T., Bumby, A.J., Catuneanu, O., Mostert, P., van der Neut, M., 2009. Possible evidence for episodic epeiric marine and fluvial sedimentation (and implications for palaeoclimatic conditions), ca. 2.3–1.8 Ga, Kaapvaal craton, South Africa. Palaeogeography, Palaeoclimatology, Palaeoecology 273, 153–173.
Evans, D.A., Beukes, N.J., Kirschvink, J.L., 1997. Low-latitude glaciation in the Palaeoproterozoic era. Nature 386, 262–266.
Evans, D.A.D., 2003. A fundamental Precambrian–Phanerozoic shift in earth's glacial style? Tectonophysics 375, 353–385.
Eyles, N., 2008. Glacioepochs and the supercontinent cycle after ~3.0 Ga: tectonic boundary conditions for glaciations. Palaeogeography, Palaeoclimatology, Palaeoecology 258, 89–129.
Fairchild, I.J., Kennedy, M.J., 2007. Neoproterozoic glaciation in the Earth System. Journal of the Geological Society 164, 895–921.
Farquhar, J., Bao, H., Thiemens, M., 2000. Atmospheric influence of Earth's earliest sulfur cycle. Science 289, 756–758.
Farquhar, J., Namping, W., Canfield, D.E., Oduro, H., 2010. Connections between sulfur cycle evolution, sulfur isotopes, sediments, and base metal sulfide deposits. Economic Geology 105, 509–533.
Frakes, L.A., 1979. Climates Throughout Geologic Time. Elsevier, Amsterdam, 310 pp.
Fralick, P.W., Miall, A.D., 1989. Sedimentology of the lower Huronian Supergroup (Early Proterozoic), Elliot Lake area, Ontario, Canada. Sedimentary Geology 63, 127–153.
Frauenstein, F., Veizer, J., Beukes, N., van Niekerk, H.S., Coetzee, L.L., 2009. Transvaal Supergroup carbonates: implications for Paleoproterozoic $\delta^{18}O$ and $\delta^{13}C$ records. Precambrian Research 175, 149–160.
Frei, R., Gaucher, C., Poulton, S.W., Canfield, D.E., 2009. Fluctuations in Precambrian atmospheric oxygenation recorded by chromium isotopes. Nature 461, 250–253.
Goldblatt, C., Lenton, T.M., Watson, A.J., 2006. Bistability of atmospheric oxygen and the Great Oxidation. Nature 443, 683–686.
Gutzmer, J., Beukes, N.J., 1998. High grade manganese ores in the Kalahari manganese field: characterization and dating of the oreforming events. Unpublished Report. Rand Afrikaans University, Johannesburg, 221 pp.
Halls, H.C., Bates, M.P., 1990. The evolution of the 2.45 Ga Matachewan dyke swarm, Canada. In: Parker, A.J., Rickwood, P.C., Tucker, D.H. (Eds.), Mafic Dykes and Emplacement Mechanism, pp. 237–249.
Hambrey, M.J., Harland, W.B. (Eds.), 1981. Earth's Pre-pleistocene Glacial Record. Cambridge University Press, Cambridge, 1004 pp.
Hamilton, J., 1977. Sr isotope and trace element studies of the Great Dyke and Bushveld mafic phase and their relation to early Proterozoic magma genesis in southern Africa. Journal of Petrology 18, 24–52.
Hammond, R.D., 1976. Geochronology and origin of Archean rocks in Marquette County, Upper Michigan. M.S. Thesis. University of Kansas, Lawrence, 108 pp.
Hannah, J.L., Bekker, A., Stein, H.J., Markey, R.J., Holland, H.D., 2004. Primitive Os and 2316 Ma age for marine shale: implications for Paleoproterozoic glacial events and the rise of atmospheric oxygen. Earth and Planetary Science Letters 225, 43–52.
Hanski, E., Huhma, H., Vaasjoki, M., 2001. Geochronology of northern Finland: a summary and discussion. In: Vaasjoki, M. (Ed.), Radiometric Age Determination from Finnish Lapland and Their Bearing on the Timing of Precambrian Volcanosedimentary Sequences. Geological Survey of Finland Bulletin Special Paper 33, pp. 255–279.
Heaman, L.M., 1997. Global mafic volcanism at 2.45 Ga: remnants of an ancient large igneous province? Geology 25, 299–302.
Herz, N., Dutra, C.V., 1964. Geochemistry of some kyanites from Brazil. The American Mineralogist 49, 1290–1305.
Hoffman, P.F., Kaufman, A.J., Halverson, G.P., Schrag, D.P., 1998. A Neoproterozoic snowball Earth. Science 281, 1342–1346.
Holland, H.D., 1994. Early Proterozoic atmospheric change. In: Bengston, S. (Ed.), Early Life on Earth. Nobel Symposium No. 84. Columbia University Press, New York, pp. 237–244.
Holland, H.D., 2002. Volcanic gases, black smokers, and the great oxidation event. Geochimica et Cosmochimica Acta 66, 3811–3826.
Holland, H.D., 2009. Why the atmosphere became oxygenated: a proposal. Geochimica et Cosmochimica Acta 73, 5241–5255.
Huhma, H., 1986. Sm–Nd and Pb–Pb isotopic evidence for the origin of the Early Proterozoic Svecokarelian crust in Finland. Geological Survey of Finland Bulletin 337, 48.
Jones, D.L., Robertson, D.M., McFadden, P.L., 1975. A palaeomagnetic study of Precambrian dyke swarms associated with the Great Dyke of Rhodesia. Transactions of the Geological Society of South Africa 78, 57–65.
Karhu, J.A., 1993. Paleoproterozoic evolution of the carbon isotope ratios of sedimentary carbonates in the Fennoscandian Shield. Geological Survey of Finland Bulletin 371, 87.
Karhu, J.A., Holland, H.D., 1996. Carbon isotopes and the rise of atmospheric oxygen. Geology 24, 867–870.
Karlstrom, K.E., Flurkey, A.J., Houston, R.S., 1983. Stratigraphy and depositional setting of the Proterozoic Snowy Pass Supergroup, southeastern Wyoming: record of a Paleoproterozoic Atlantic-type cratonic margin. Geological Society of America Bulletin 94, 1257–1274.
Kasting, J.E., 2004. When methane made climate. Scientific American 291, 78–85.
Kasting, J.E., 2005. Methane and climate during the Precambrian era. Precambrian Research 137, 119–129.
Kasting, J.F., 2001. The rise of atmospheric oxygen. Science 293, 819–820.
Kasting, J.F., Siefert, J.L., 2002. Life and the evolution of Earth's atmosphere. Science 296, 1066–1068.
Kaufman, A.J., Johnston, D.T., Farquhar, J., Masterson, A.L., Lyons, T.W., Bates, S., Anbar, A.D., Arnold, G.L., Garvin, J., Buick, R., 2007. Late Archean biospheric oxygenation and atmospheric evolution. Science 317, 1900–1903.
Kirschvink, J.L., Gaidos, E.J., Bertani, L.E., Beukes, N.J., Gutzmer, J., Maepa, L.N., Steinberger, R.E., 2000. Paleoproterozoic snowball Earth: extreme climatic and geochemical global change and its biological consequences. Proceedings of the National Academy of Sciences of the United States of America 97, 1400–1405.
Konhauser, K.O., Lalonde, S.V., Planavsky, N.J., Pecoits, E., Lyons, T.W., Mojzsis, S.J., Rouxel, O.J., Barley, M.E., Rosìere, C., Fralick, P.W., Kump, L.R., Bekker, A., 2011. Aerobic bacterial pyrite oxidation and acid rock drainage during the Great Oxidation Event. Nature 478, 369–373.
Konhauser, K.O., Pecoits, E., Lalonde, S.V., Papineau, D., Nisbet, E.G., Barley, M.E., Arndt, N.T., Zahnle, K., Kamber, B.S., 2009. Oceanic nickel depletion and a methanogen famine before the Great Oxidation Event. Nature 458, 750–753.
Kopp, R.E., Kirschvink, J.L., Hilburn, I.A., Nash, C.Z., 2005. The Paleoproterozoic snowball Earth: a climatic disaster triggered by the evolution of oxygenic photosynthesis. Proceedings of the National Academy of Sciences of the United States of America 102, 11131–11136.
Krogh, T.E., Davis, D.W., Corfu, F., 1984. Precise U–Pb zircon and baddeleyite ages for the Sudbury area. In: Pye, E.G., Naldrett, A.J., Giblin, P.E. (Eds.), The Geology and Ore Deposits of the Sudbury Structure. Ontario Geological Survey, vol. 1, pp. 431–446.
Lai, Y., Chen, C., Tang, H.S., 2012. Paleoproterozoic positive $\delta^{13}C$ excursion in Henan, China. Geomicrobiology Journal 29, 287–298.
Latypov, R.M., Mitrofanov, F.P., Alapieti, T.T., Kaukonen, R.J., 1999. Petrology of Upper Layered Horizon (ULH) of West-Pansky intrusion, Kola Peninsula, Russia. Geology and Geophysics 40, 1434–1456.
Lindsay, J.F., Brasier, M.D., 2002. Did global tectonics drive early biosphere evolution? Carbon isotope record from 2.6 to 1.9 Ga carbonates of Western Australian basins. Precambrian Research 114, 1–34.

Long, D.G.F., 2004. The tectonostratigraphic evolution of the Huronian basement and subsequent basin fill: geological constraints on impact models of the Sudbury event. Precambrian Research 129, 203–223.
Lyons, T.W., Reinhard, C.T., 2009. Early Earth: oxygen for heavy-metal fans. Nature 461, 179–181.
Machado, N., Carneiro, M.A., 1992. U–Pb evidence of late Archean tectono-thermal activity in the southern São Francisco shield, Brazil. Canadian Journal of Earth Sciences 29, 2341–2346.
Machado, N., Noce, C.M., Ladeira, E.A., Belo de Oliveira, O., 1992. U–Pb geochronology of Archean magmatism and Proterozoic metamorphism in the Quadrilátero Ferrífero, southern São Francisco craton, Brazil. Geological Society of America Bulletin 104, 1221–1227.
Machado, N., Schrank, A., Noce, C.M., Gauthier, G., 1996. Ages of detrital zircon from Archean–Paleoproterozoic sequences: implications for greenstone belt setting and evolution of a Transamazonian foreland basin in Quadrilátero Ferrífero, southeast Brazil. Earth and Planetary Science Letters 141, 259–276.
Marmo, J.S., Ojakangas, R.W., 1984. Lower Proterozoic glaciogenic deposits, eastern Finland. Geological Society of America Bulletin 95, 1055–1062.
Marmo, J.S., 1992. The lower Proterozoic Hokkalampi paleosol in north Karelia, eastern Finland. In: Schidlowski, M., Golubic, S., Kimberley, M.M., Trudinger, P.A. (Eds.), Early Organic Evolution: Implication for Mineral and Energy Resources. Springer, Berlin, pp. 41–66.
Marshak, S., Alkmim, F.F., 1989. Proterozoic contraction/extension tectonics of the southern São Francisco region, Minas Gerais, Brazil. Tectonics 8, 555–571.
Martin, D.M., 1999. Depositional setting and implications of Paleoproterozoic glaciomarine sedimentation in the Hamersley Province, Western Australia. Geological Society of America Bulletin 111, 189–203.
Martin, D.M., Clendenin, C.W., Krapez, B., McNaughton, N.J., 1998. Tectonic and geochronological constraints on late Archaean and Palaeoproterozoic stratigraphic correlation within and between the Kaapvaal and Pilbara Cratons. Journal of the Geological Society of London 155, 311–322.
Maxwell, C.H., 1972. Geology and ore deposits of the Alegria District, Minas Gerais, Brazil. United States Geological Survey Professional Paper 341-J, 72 pp.
Melezhik, V.A., 2006. Multiple causes of Earth's earliest global glaciation. Terra Nova 18, 130–137.
Melezhik, V.A., Fallick, A.E., 1996. A widespread positive $\delta^{13}C_{carb}$ anomaly at 2.33–2.06 Ga on the Fennoscandian Shield: a paradox? Terra Nova 8, 141–157.
Melezhik, V.A., Fallick, A.E., Makarikhin, V.V., Lubtsov, V.V., 1997a. Links between Palaeoproterozoic palaeogeography and rise and decline of stromatolites: Fennoscandian Shield. Precambrian Research 82, 311–348.
Melezhik, V.A., Fallick, A.E., Semikhatov, M.A., 1997b. Could stromatolite-forming cyanobacteria have influenced the global carbon cycle at 2300–2060 Ma? Norges Geologiske Undersøkelse Bulletin 433, 30–31.
Melezhik, V.A., Fallick, A.E., Filippov, M.M., Larsen, O., 1999a. Karelian shungite—an indication of 2.0-Ga-old metamorphosed oil-shale and generation of petroleum: geology, lithology and geochemistry. Earth-Science Reviews 47, 1–40.
Melezhik, V.A., Fallick, A.E., Medvedev, P.V., Makarikhin, V.V., 1999b. Extreme $^{13}C_{carb}$ enrichment in ca. 2.0 Ga magnesite–stromatolite–dolomite–'red beds' association in a global context: a case for the worldwide signal enhanced by a local environment. Earth-Science Reviews 48, 71–120.
Melezhik, V.A., Sturt, B.A., 1994. General geology and evolutionary history of the early Proterozoic Polmak–Pasvik–Pechenga–Imandra/Varzuga–Ust'Ponoy greenstone belt in the northeastern Baltic Shield. Earth-Science Reviews 36, 205–241.
Mertanen, S., Pesonen, L.J., Huhma, H., Leino, M.A.H., 1989. Palaeomagnetism of the Early Proterozoic layered intrusions, northern Finland. Geological Survey of Finland Bulletin 347, 1–40.
Miall, A.D., 1983. Glaciomarine sedimentation in the Gowganda Formation (Huronian), northern Ontario. Journal of Sedimentary Research 53, 477–491.
Morey, G.B., Southwick, D.L., 1995. Allostratigraphic relationships of early Proterozoic iron-formations in the Lake Superior region. Economic Geology 90, 1983–1993.
Mossman, D.J., Harron, G.A., 1983. Origin and distribution of gold in the Huronian Supergroup, Canada: the case for Witwatersrand type paleoplacers. Precambrian Research 20, 543–583.
Nesbitt, H.W., Young, G.M., 1982. Early Proterozoic climates and plate motions inferred from major element chemistry of lutites. Nature 299, 715–717.
Noce, C.M., Machado, N., Teixeira, W., 1998. U–Pb geochronology of gneisses and granitoids in the Quadrilátero Ferrífero (southern São Francisco craton): age constraints from Archean and Paleoproterozoic magmatism and metamorphism. Revista Brasileira de Geociências 28, 95–102.
Ojakangas, R.W., 1988. Glaciation: an uncommon "mega-event" as a key to intracontinental and intercontinental correlation of Early Proterozoic basin fill, North American and Baltic cratons. In: Kleinspehn, K.L., Paola, C. (Eds.), New Perspectives in Basin Analysis. Springer, New York, pp. 431–444.
Ojakangas, R.W., Marmo, J.S., Heiskanen, K., 2001. Basin evolution of the Paleoproterozoic Karelian Supergroup of the Fennoscandian (Baltic) Shield. Sedimentary Geology 141–142, 255–285.
Panahi, A., Young, G.M., Rainbird, R.H., 2000. Behaviour of major and trace elements (including REE) during Paleoproterozoic pedogenesis and diagenetic alteration of an Archean granite near Ville Marie, Quebec, Canada. Geochimica et Cosmochimica Acta 64, 2199–2220.
Pavlov, A.A., Kasting, J.F., 2002. Mass-independent fractionation of sulfur isotopes in Archean sediments: strong evidence for an anoxic Archean atmosphere. Astrobiology 2, 27–41.
Pavlov, A.A., Kasting, J.F., Brown, L.L., 2000. Greenhouse warming by CH_4 in the atmosphere of early Earth. Journal of Geophysical Research 105, 11981–11990.
Pekkarinen, L.J., Lukkarinen, H., 1991. Palaeoproterozoic volcanism in the Kiihtelysvaara–Tohmajärvi district, eastern Finland. Geological Survey of Finland Bulletin 357, 30.
Pickard, A.L., 2002. SHRIMP U–Pb zircon ages of tuffaceous mudrocks in the Brockman Iron Formation of the Hamersley Range, Western Australia. Australian Journal of Earth Sciences 49, 491–507.
Pickard, A.L., 2003. SHRIMP U–Pb zircon ages for the Palaeoproterozoic Kuruman Iron Formation, Northern Cape Province, South Africa: evidence for simultaneous BIF deposition on Kaapvaal and Pilbara Cratons. Precambrian Research 125 (3/4), 275–315.
Polteau, S., Moore, J.M., Tsikos, H., 2006. The geology and geochemistry of the Palaeoproterozoic Makganyene diamictite. Precambrian Research 148, 257–274.
Prasad, N., Roscoe, S.M., 1996. Evidence of anoxic to oxic atmospheric change during 2.45–2.22 Ga from lower and upper sub-Huronian paleosols, Canada. Catena 27, 105–121.
Premo, W.R., Van Schmus, W.R., 1989. Zircon geochronology of Precambrian rocks in southeastern Wyoming and northern Colorado. In: Grambling, J.A., Tewksbury, B.J. (Eds.), Proterozoic Geology of the Southern Rocky Mountains. Geological Society of America Special Paper 235, pp. 1–12.
Puchtel, I.S., Haase, K.M., Hofmann, A.W., Chauvel, C., Kulikov, V.S., Garbe-Schönberg, C.D., Nemchin, A.A., 1997. Petrology and geochemistry of crustally contaminated komatiitic basalts from the Vetreny Belt, southeastern Baltic Shield: evidence for an early Proterozoic mantle plume beneath rifted Archean continental lithosphere. Geochimica et Cosmochimica Acta 61, 1205–1222.
Puchtel, I.S., Hofmann, A.W., Mezger, K., Schipansky, A.A., Kulikov, V.S., Kulikova, V.V., 1996. Petrology of a 2.41 Ga remarkably fresh komatiitic basalt lava lake in Lion Hills, central Vetreny Belt, Baltic Shield. Contributions to Mineralogy and Petrology 124, 273–290.
Rainbird, R.H., Davis, W.J., 2006. Sampling superior: detrital zircon geochronology of the Huronian. Geological Association of Canada Abstracts with Programs 31, 125.
Rainbird, R.H., Nesbitt, H.W., Donaldson, J.A., 1990. Formation and diagenesis of a sub-Huronian saprolith: comparison with a modern weathering profile. Journal of Geology 98, 801–822.
Raymo, M.E., 1991. Geochemical evidence supporting T.C. Chamberlin's theory of glaciation. Geology 19, 344–347.
Romano, A.W., 1989. Evolution tectonique de la region Nord-Ouest du Quadrilatere Ferrifere – Minas Gerais – Bresil (Geochronologie du socle – aspects geochimiques et petrographiques des supergroupes Rio Das Velhas et Minas). Ph.D. thesis, Université de Nancy I, Nancy, France, 259 pp.
Rye, R., Holland, H.D., 1998. Paleosols and the evolution of atmospheric oxygen: a critical review. American Journal of Science 298, 621–672.
Schidlowski, M., 1988. A 3800-million-year isotopic record of life from carbon in sedimentary rocks. Nature 333, 313.
Schidlowski, M., Eichmann, R., Junge, C.E., 1975. Precambrian sedimentary carbonates: carbon and oxygen isotope geochemistry and implications for the terrestrial oxygen budget. Precambrian Research 2, 1–69.
Schidlowski, M., Eichmann, R., Junge, C.E., 1976. Carbon isotope geochemistry of the Precambrian Lomagundi carbonate province, Rhodesia. Geochimica et Cosmochimica Acta 40, 449–455.
Sekine, Y., Tajika, E., Tada, R., Hirai, T., Goto, K.T., Kuwatani, T., Goto, K., Yamamoto, S., Tachibana, S., Isozaki, S.Y., Kirschvink, J.L., 2011. Manganese enrichment in the Gowganda Formation of the Huronian Supergroup: a highly oxidizing shallow-marine environment after the last Huronian glaciation. Earth and Planetary Science Letters 307, 201–210.
Simonson, B.M., Schubel, K.A., Hassler, S.W., 1993. Carbonate sedimentology of the early Precambrian Hamersley Group of Western Australia. Precambrian Research 60, 287–335.
Strand, K., 2012. Global and continental-scale glaciations on the Precambrian earth. Marine and Petroleum Geology 33, 69–79.
Strand, K., Laajoki, K., 1993. Palaeoproterozoic glaciomarine sedimentation in an extensional tectonic setting: the Honkala Formation, Finland. Precambrian Research 64, 253–271.
Strauss, H., Des Marais, D.J., Hayes, J.M., Summons, R.E., 1992. The carbon-isotopic record. In: Schopf, J.W., Klein, C. (Eds.), The Proterozoic Biosphere: A Multidisciplinary Study. Cambridge University Press, New York, pp. 117–127.
Sturt, B.A., Melezhik, V.A., Ramsay, D.M., 1994. Early Proterozoic regolith at Pasvik, NE Norway: palaeoenvironmental implications for the Baltic Shield. Terra Nova 6, 618–633.
Sundquist, E.T., 1993. The global carbon dioxide budget. Science 259, 934–941.
Tang, G.J., Chen, Y.J., Huang, B.L., Chen, C.X., 2004. Paleoproterozoic $\delta^{13}C_{carb}$ positive excursion event: research progress on 2.3 Ga catastrophe. Journal of Mineralogy and Petrology 24 (3), 103–109 (in Chinese with English abstract).
Tang, H.S., Chen, Y.J., Santosh, M., Yang, T., 2012. REE geochemistry of carbonates from the Guanmenshan Formation, Liaohe Group, NE Sino-Korean Craton: implications for seawater compositional change during the Great Oxidation Event. Precambrian Research 227, 316–336.
Tang, H.S., Chen, Y.J., Santosh, M., Zhong, H., Wu, G., Lai, Y., 2013. C–O isotope geochemistry of the Dashiqiao magnesite belt, North China Craton: implications for the Great Oxidation Event and ore genesis. Geological Journal. http://dx.doi.org/10.1002/gj.2486.

Tang, H.S., Chen, Y.J., Wu, G., Lai, Y., 2011. Paleoproterozoic positive $\delta^{13}C_{carb}$ excursion in northeastern Sino-Korean craton: evidence of the Lomagundi Event. Gondwana Research 19, 471–481.
Tankard, A.J., Jackson, M.P.A., Eriksson, K.A., Hobday, D.K., Hunter, D.R., Minter, W.E.L., 1982. Crustal Evolution of Southern Africa. Springer, New York, 523 pp.
Taylor, A.S., Lasaga, A.C., 1999. The role of basalt weathering in the Sr isotope budget of the oceans. Chemical Geology 161, 199–214.
Taylor, S.R., McLennan, S.M., 1985. The Continental Crust: Its Composition and Evolution. Blackwell, Oxford, 312 pp.
Trendall, A.F., 1990. Hamersley BasinGeology and Mineral Resources of Western Australia. Western Australian Geological Survey Memoir 3, 163–190.
Trendall, A.F., Blockley, J.G., 1970. The iron formations of the Precambrian Hamersley Group, Western Australia, with special reference to the associated crocidolite. Western Australian Geological Survey Bulletin 119, 366.
Trendall, A.F., Nelson, D.R., de Laeter, J.R., Hassler, S.W., 1998. Precise zircon U–Pb ages from the Marra Mamba Iron Formation and the Wittenoom Formation, Hamersley Group, Western Australia. Australian Journal of Earth Sciences 45, 137–142.
Tyler, I.M., Thorne, A.M., 1990. The northern margin of the Capricorn Orogen, Western Australia—an example of an early Proterozoic collision zone. Journal of Structural Geology 12, 685–701.
Vallini, D.A., Cannon, W.F., Schulz, K.J., 2006. New constraints on the timing of Paleoproterozoic glaciation, Lake Superior region: detrital zircon and hydrothermal xenotime ages on the Chocolay Group, Marquette Range Supergroup. Canadian Journal of Earth Sciences 43, 571–591.
Voegelin, A.R., Nägler, T.F., Beukes, N.J., Lacassie, J.P., 2010. Molybdenum isotopes in late Archean carbonate rocks: implications for early Earth oxygenation. Precambrian Research 182, 70–82.
Vogel, D.C., Vuollo, J.I., Alapieti, T.T., James, R.S., 1998. Tectonic, stratigraphic, and geochemical comparison between ca. 2500–2440 Ma mafic igneous events in the Canadian and Fennoscandian Shields. Precambrian Research 92, 89–116.
Walraven, F., 1997. Geochronology of the Rooiberg Group, Transvaal Supergroup, South Africa. Economic Geology Research Unit, University of the Witwatersrand, Johannesburg, South Africa. Inf. Circ. 316, 21 pp.
Walraven, F., Armstrong, R.A., Kruger, F.J., 1990. A chronostratigraphic framework for the north-central Kaapvaal craton, the Bushveld complex, and the Vredefort structure. Tectonophysics 171, 23–48.
Wille, M., Kramers, J.D., Nägler, T.F., Beukes, N.J., Schröder, S., Meisel, Th., Lacassie, J.P., Voegelin, A.R., 2007. Evidence for a gradual rise of oxygen between 2.6 and 2.5 Ga from Mo isotopes and Re-PGE signatures in shales. Geochimica et Cosmochimica Acta 71, 2417–2435.
Williams, H., Hoffman, P.F., Lewry, J.F., Monger, J.W.H., Rivers, T., 1991. Anatomy of North America: thematic portrayals of the continent. Tectonophysics 187, 117–134.
Young, G.M., 1970. An extensive early Proterozoic glaciation in North America. Palaeogeography, Palaeoclimatology, Palaeoecology 7, 85–101.
Young, G.M., 1973. Tillites and aluminous quartzites as possible time markers for Middle Precambrian (Aphebian) rocks of North America. In: Young, G.M. (Ed.), Huronian Stratigraphy and Sedimentation. The Gelogical Association of Canada Special Paper 12, pp. 97–127.
Young, G.M., 1991. The geological record of glaciation: relevance to the climatic history of the Earth. Geoscience Canada 18 (3), 100–108.
Young, G.M., 2002. Stratigraphic and tectonic settings of Proterozoic glaciogenic rocks and banded iron-formations: relevance to the snowball Earth debate. Journal of Africa Earth Sciences 35, 451–466.
Young, G.M., 2012. Secular changes at the Earth's surface: evidence from palaeosols, some sedimentary rocks, and palaeoclimatic perturbations of the Proterozoic Eon. Gondwana Research. http://dx.doi.org/10.1016/j.gr.2012.07.016.
Young, G.M., 2013. Precambrian supercontinents, glaciations, atmospheric oxygenation, metazoan evolution and an impact that may have changed the second half of Earth history. Geoscience Frontiers 4, 247–261.
Young, G.M., Long, D.G.F., Fedo, C.M., Nesbitt, H.W., 2001. Paleoproterozoic Huronian basin: product of a Wilson cycle punctuated by glaciations and a meteorite impact. Sedimentary Geology 141–142, 233–254.
Young, G.M., Nesbitt, H.W., 1985. The Gowganda Formation in the southern part of the Huronian outcrop belt, Ontario, Canada: stratigraphy, depositional environments and regional tectonic significance. Precambrian Research 29, 265–301.
Zhai, M.G., Santosh, M., 2013. Metallogeny in the North China Craton: secular changes in the evolving Earth. Gondwana Research 24, 275–297.
Zhao, Z.H., 2010. Banded iron formation and great oxidation event. Earth Science Frontiers 17, 1–12 (in Chinese with English abstract).
Zhong, H., Hu, R.Z., Zhu, W.G., Liu, B.G., 2007. Genesis and mineralization of layered intrusions. Earth Science Frontiers 14, 159–172 (in Chinese with English abstract).

Haoshu Tang is an associate professor at the Institute of Geochemistry, Chinese Academy of Sciences, B.E. (1998) from Guizhou University of Technology (China), and Ph.D. (2010) from Peking University. Her professional field is Mineralogy, Petrology and Mineral Deposits. Her major research interest is ore geology and geochemistry, Precambrian geology and geochemistry.

Yanjing Chen is a professor at the Peking University (Beijing) and also at the Guangzhou Institute of Geochemistry, Chinese Academy of Sciences, B.S. (1984), M.S. (1987) and Ph.D. (1990) from Nanjing University (China). Research fields include economic geology, fluid inclusion, geochemistry, Precambrian geology, ore exploration, and continental collision orogeny. Published over 200 research papers and the book “Gold Mineralization in Western Henan” (Chinese Seismological Press, 1992, in Chinese). Also edited several memoir volumes and journal special issues.